Title: Assessment of AAV vector tropisms for mouse and human pluripotent stem cell-derived RPE and photoreceptor cells.

Authors: Anai Gonzalez-Cordero[1,$], Debbie Goh[1,$], Kamil Kruczek[1], Arifa Naeem[1], Milan Fernando[1], Sophia-Martha kleine Holthaus[1,2], Matsuki Takaaki[1], Samuel J. I. Blackford[1], Magdalena Kloc[1], Leticia Agundez[1], Robert D. Sampson[1], Shyamanga Borooah[3], Patrick Ovando-Roche[1], Manjit S. Mehat[1], Emma L. West[1], Alexander J. Smith[1], Rachael A. Pearson[1], Robin R. Ali[1].

Address: [1] UCL, Department of Genetics, Institute of Ophthalmology, 11-43 Bath Street, London, EC1V 9EL UK

[2] UCL, MRC Laboratory for Molecular Cell Biology, Gower Street, London, WC1E 6BT UK

[3] Centre for Clinical Brain Sciences, University of Edinburgh, Edinburgh EH16 4SB UK

$ These authors contributed equally

Correspondence: Robin Ali (r.ali@ucl.ac.uk)

Short title: AAV tropism in stem cell-derived retinal cultures

Abstract

Adeno-associated viral vectors are showing great promise as gene therapy vectors for a wide range of retinal disorders. To date, evaluation of therapeutic approaches has depended almost exclusively on the use of animal models. With recent advances in human stem cell technology, stem-cell derived retina now offers the possibility to assess efficacy in human organoids *in vitro*. Here we test 6 AAV serotypes (AAV2/2, AAV2/9, AAV2/8, AAV2/8T(Y733F), AAV2/5 and ShH10) to determine their efficiency in transducing mouse and human pluripotent stem cell (PSC)-derived RPE and photoreceptor cells *in vitro*. All the serotypes tested were capable of transducing RPE and photoreceptor cells *in vitro*. AAV ShH10 and AAV2/5 are the most efficient vectors at transducing both mouse and human RPE, while AAV2/8 and ShH10 achieved similarly robust transduction of human ESC-derived cone photoreceptors. Furthermore, we show that hESC-derived photoreceptors can be used to establish promoter specificity in human cells *in vitro.* The results of this study will aid capsid selection and vector design for pre-clinical evaluation of gene therapy approaches, such as gene editing, that require the use of human cells and tissues.

Key words: pluripotent stem cells; retinal organoids; AAV serotypes; gene therapy

Introduction

AAV vectors have been used in a number of clinical trials of retinal gene therapy (for recent review see Auricchio *et al.*[1]). These include seminal trials of therapies to treat childhood blindness caused by RPE65 related Leber congenital amaurosis (LCA)[2-6]. A number of different AAV vector pseudotypes exist that display distinct transduction profiles, which may be used to deliver the transgene of interest to specific cell types. Conventionally, mouse[7] and large animal models, including dogs[8,9], pigs[10-12] and primates[13,14] have been used to evaluate AAV specificity and efficiency for transducing photoreceptors and RPE *in vivo*. The *in vivo* results consistently show greater photoreceptor transduction efficiency by serotypes AAV2/5, 2/8 and 2/9, compared with the archetypal AAV2/2 vector. Recently, screening for tropism and infectivity of human retinal cells has also been performed in *ex vivo* human retinal explants, although the results appear to be highly variable between individual explants[15-17].

The availability of pluripotent stem cells (PSC) that can be effectively differentiated into 3D retinal organoids has brought many new opportunities for accelerating the development of novel therapies for wide range of retinal conditions, including inherited retinal dystrophies caused by defects in either photoreceptors or the retinal pigment epithelium (RPE). Numerous reports have described the differentiation of both mouse and human pluripotent stem cells into photoreceptors and RPE, for transplantation[18-25] and *in vitro* disease modeling studies, using patient-derived induced pluripotent stem cells (iPSCs)[26-29]. The combined use of relatively new stem cell technologies, together with the more established use of recombinant adeno-associated viral (AAV) vectors for gene therapy represents a unique opportunity for advancing our ability to understand and treat inherited retinal disorders.

A growing number of studies are utilizing PSC-derived retinal organoids and efficient gene transfer to these tissues is of increasing interest. We have previously observed that AAV vectors are more effective at mediating gene transfer than either lentiviral vectors or physical methods such as transfection or electroporation and have therefore previously used AAV vectors to mark mouse and human PSC-derived photoreceptor precursors in order to isolate and purify them for use in transplantation studies[25,30,31]. Human PSC-derived retinal organoids provide access to large numbers of normal and diseased samples and also offer a new platform to evaluate gene correction by gene therapy specifically in human retinal cells. The precise modification of the genome can be achieved by well-described gene editing technologies, such as zinc fingers, TALENS and CRISPR/Cas9[32,33]. The *in vivo* delivery of these editing tools to the mouse retina using AAV has now been demonstrated in a number of recent studies (for review see[34]). However, as a prelude to *in vivo* gene editing, double strand breaks efficiency, cutting specificity, and efficiency of gene integration, when a donor DNA is used, needs to be tested first in cells *in vitro*. Whilst various cells lines can be used, mouse and human retinal organoids provide more appropriate tools to evaluate gene editing than primary cell lines. Furthermore, in the case of patient-derived human organoids, these provide unlimited number of diseased cells to develop and test the most efficient gene correction technology. Whilst AAV vectors are promising tools for mediating gene editing in retinal organoids, it is first necessary to establish which AAV serotypes most efficiently transduce these tissues *in vitro*. This study therefore assesses the tropism of AAV vectors in stem cell-derived retinal organoids. We sought to determine the relative transduction efficiencies and toxicities of six AAV serotypes (AAV2/9, AAV2/8, AAV2/8T(Y733F), AAV2/5, AAV2/2 and ShH10(Y445F)) in mouse and human PSC-derived photoreceptor and RPE cells. These 6 serotypes were chosen for comparison *in vitro* because of their widespread use *in vivo*. AAV2/8, AAV2/2 and AAV2/5 have been used

in ocular gene therapy trials, whilst AAV2/9 and the two engineered capsids, ShH10 and AAV2/8T(Y733F), mediate particularly efficient *in vivo* transduction.

Materials and Methods

Mouse ESC retinal differentiation culture

A CCE mouse ES cell line (129/SvEv; a kind gift of Professor E. Robertson) was maintained as previously described[35]. For 3D retinal differentiation, $3x10^4$ dissociated ES cells were re-suspended per ml of differentiation medium (GMEM containing 1.5% KSR, 0.1mM NEAA, 1mM pyruvate, 0.1mM 2-mercaptoethanol), plated into 96 well low-binding (Corning) plates and incubated at 37°C, 5% CO_2. Embryoid body cell aggregates (EBs) formed within 24 hrs, on day 1 of culture, growth factor reduced Matrigel (GIBCO) was added to each well to give a final concentration of 2%. For whole EB retinal differentiation towards photoreceptor cell fate, EBs were transferred into retinal maturation medium (DMEM/F12 Glutamax containing N2 supplement and Pen/strep) at day 9, plated in low-binding plates at a density of 6 EBs/cm^2 and incubated at 37°C, 5% CO_2. The media was changed every 2-3 days, with the addition of 1mM Taurine (Sigma) and 500nM retinoic acid (Sigma) from day 14 of culture onwards. For whole EB retinal differentiation towards RPE cell fate, EBs were treated with 500nM working solution of 6-bromoindirubin-3'-oxime, BIO (Sigma), from day 5 onwards. For monolayer cultures of RPE pigmented regions of the BIO-treated EBs were manually dissected with a 21G needle and platted these on laminin coated chamber slides.

Human ESC maintenance and retinal differentiation culture

The human embryonic and iPS stem cell lines (H9 and IRM90-4 from Wicell) were maintained on feeder free conditions on E8 and geltrex coated 6 well plates. RPE differentiation protocol

was adapted from previous published protocols[19,36]. Briefly, hPSCs were dissociated using a dispase and collagenase solution. PSC clumps were collected and re-suspended in E8 media. The cell clumps were then transferred to a low-binding 10 cm plate to form floating EBs. Differentiation media was changed to EB media (DMEM/F12 (1:1), Knockout serum replacement, MEM non-essential amino acids, L glutamine, 2-Mercaptoethanol, Pen/Strep) containing 100ng/ml of dorsomorphin (BMP inhibitor) and 100ng/ml of XAV939 (DKK1-Wnt inhibitor) from day 2 to 3 of culture. From day 4 of culture media was changed to neural induction media (Advanced DMEM/F12, MEM non-essential amino acids, N2, Heparin and Pen/Strep). On day 7 EBs were platted on laminin for growth as adherent cultures. From day 15 media was changed to retinal maturation media (DMEM, F12, B27 without retinoic acid and Pen/Strep) containing 50 ng/ml of Activin A (R&D) was added from day 18 to 40. Islands of pigmented RPE appeared between day 40-60 and these regions were manually dissected for further expansion and quantification on laminin-coated wells.

For retinal neuroepithelia differentiation we used a previously described protocol[25]. Briefly, human PSCs were maintained until confluent when media without FGF was added to cultures for two days. Proneural induction media (Advanced DMEM/F12, MEM non-essential amino acids, N2 Supplement, 100mM Glutamine and Pen/Strep) was added until optic vesicles were observed. Vesicles were manually excised and kept in 96 well plates in retinal differentiation media (DMEM, F12, Pen/Strep and B27 without retinoic acid) and at 6 weeks of differentiation medium was supplemented with FBS, taurine and glutamax and at 10 weeks RA was added.

Production of recombinant AAV serotypes and in vitro *transduction analysis*

A pD10/CMV promoter-*GFP,* construct containing AAV-2 inverted terminal repeat (ITR) was used to generate AAV2/9, AAV2/8, AAV2/8(Y733F), AAV2/5, AAV2/2 and ShH10(Y445F) CMV.GFP viruses. A pD10/Rhodopsin *promoter-GFP and a* pD10/2.1PRM/L-opsin *promoter-*

GFP was used to generate viruses. Recombinant AAV2/2 serotype particles were produced through a previously described triple transient transfection method HEK293T cells(37). AAV2/8, AAV2/8(Y733F), AAV2/5, AAV2/2 and ShH10(Y445F) serotypes were bound to an AVB Sepharose column (GE Healthcare), and eluted with 50 mM Glycine pH2.7 into 1 M Tris pH 8.8. AAV2/9 was purified by size separation on a Sephacryl S300 column, followed by anion exchange chromatography using a POROS 50 HQ column, eluting the vector in 20 mM Bis-Tris propane, 20 mM Trizma Base and 0.24 M NaCl pH9. Vectors were washed in 1 × PBS and concentrated to a volume of 100–150 µl using Vivaspin 4 (10 kDa) concentrators. Viral genome titres were determined by quantitative real-time PCR using a probe-based assay binding the SV40 poly-adenylation signal. Amplicon-based standard series of known amounts were used for sample interpolation. Final titres were expressed as vg/mL.

SV40 Forward primer: 5'-AGCAATAGCATCACAAATTTCACAA-3'.
SV40 Reverse primer: 5'-AGATACATTGATGAGTTTGGACAAAC-3'.
SV40 Probe: FAM-5'-AGCATTTTTTTCACTGCATTCTAGTTGTGGTTTGTC-3'-TAMRA.

The same number of EBs or RPE cells per well were used in all experiments (approximately 1.5x 10^6 EB cells and 2x10^6 RPE cells per well) and infected with 1.2x10^{11} viral particles per well in appropriated retinal medium. Estimated gMOI of 8000 and 6000.

Flow cytometry analysis

For flow cytometry experiments, mouse whole EBs (wEBs) were dissociated at day 29 of culture into a single cell suspension using a modified protocol using reagents from the papain-based Neurosphere Dissociation Kit (Miltenyi Biotec). Cells were counted and resuspended in 1% Bovine Serum Albumin (in PBS) to a concentration of 1x10^7 cells per mL, and staining was performed with 100µL aliquots. For surface marker analysis, an antibody against mouse CD73

(APC-conjugated rat IgG1, clone TY/11.8, Miltenyi Biotec) was added at a 1:75 dilution and incubated for 30 minutes at 4^{o}C. Cells were washed once in 1x Binding Buffer (eBioscience). For subsequent viability analysis, Annexin V-eFluor 450 (eBioscience) was added to samples at a 1:20 dilution (in 1X Binding Buffer) and incubated for 15 minutes at room temperature. Cells were washed once in 1X Binding Buffer and resuspended in PBS. DRAQ7 (BloStatus) was then added to the samples at a final concentration of 50ng/ml for 5 minutes at room temperature before analysis.

Cells were analysed using FlowJo software. Background fluorescence was measured using unstained cells and single-stained controls were used to set gating parameters between positive and negative populations. Small debris, cell fragments and aggregates were excluded from analysis on the basis of Annexin V and live-dead dye non-fluorescence (double negative population), followed by forward and side scatter (measuring cell size and granularity respectively). For cell surface marker analysis, dead cells were excluded from analysis on the basis of live-dead dye fluorescence as well.

For cell sorting experiments FACS was performed on a BD Influx Cell Sorter^{TM} (BD Biosciences) fitted with a 200mW 488nm blue laser to excite GFP. GFP was collected using the 488-530/40nm detector. A 70 micron nozzle at 30 psi was used and cells were collected on a 1:1 FBS/ EBSS solution.

Immunohistochemistry

For wEBs and BIO-treated wEBs experiments titre matched viruses were added at day 22 of differentiation and wEBs were collected for immunohistochemistry analysis at day 29 of culture. For adherent cultures of RPE, viruses were added between day 20 and 22 and chamber slides were fixed 7 days later. Whole EBs and eye cups were fixed for 1 hour in 4% paraformaldehyde

(PFA) and embedded in OCT (RA Lamb). Cryosections were cut (18 µm thick) and all sections were collected for analysis. For immunohistochemistry, sections were blocked in 5% goat serum and 1% bovine serum albumin in PBS. Primary antibody (**Supplementary Table 1**) was incubated overnight at 4°C. Sections were incubated with secondary antibody for 2 hrs at RT, washed and counter-stained with DAPI. Alexa fluor 488, 546 and 633 secondary antibodies were used at a 1:500 dilution.

Image acquisition

Images were acquired by confocal microscopy (Leica DM5500Q). A series of XY optical sections, approximately 1.0µm apart, throughout the depth of the section were taken and built into a stack to give a projection image. LAS AF image software was used.

Statistical analysis

All means are presented ± SD (standard deviation), unless otherwise stated; N, number of animals or independent experiments performed; n, number of eyes or EBs examined, where appropriate. For quantification assessment by Flow cytometry and cell counting of transduction efficiency, statistical analysis is based on at least three independent experiments. Statistical significance was assessed using Graphpad Prism 6 software and denoted as $P<0.05$= *, $P<0.01$= ** and $P<0.001$= ***. Appropriate statistical tests were applied including t-test; ANOVA with Tukey's correction for multiple comparisons.

Results

AAV transduction of mouse PSC-retinal cells

AAV transduction of mouse ESC-derived whole embryoid bodies (wEBs)

First, we sought to determine how efficiently we could transduce retinal organoids using AAV vectors. We have described previously the 3D-differentiation of retinal cells from mouse ESC-derived (mESC) wEBs. These structures contain both neural and glial cells, as well as retinal neuroepithelium containing mostly photoreceptors and fewer less well-developed retinal interneurons (30). We tested six different AAV serotypes, each driving eGFP under the control of a CMV promoter. A schematic of the 3D differentiation and vector transduction protocol is shown in **Fig. 1a**. At day 22 of differentiation, titre-matched AAV vectors ($1.2x10^{11}$ vg/well) were added to wEB cultures (6 wEBs in 0.3 mL medium) and the presence of GFP+ cells was assessed 7 days later. The AAV serotypes exhibited different patterns of tropism *in vitro* (**Figs. 1b-g**). Low magnification images of wEB sections at day 29 of culture showed GFP+ cells not only in regions of retinal neuroepithelium (**Fig. 1b**, arrow head), but also in other regions of the wEBs (**Fig. 1b**, arrow). The number of GFP+ transduced cells was analysed by flow cytometry. The percentage of GFP+ cells was significantly higher (53% ± 8.7) following transduction by ShH10 than by the other serotypes tested. AAV2/9 (16% ± 7.5), AAV2/8 (20% ± 4), AAV2/8T (16% ± 1.3) and AAV2/5 (12% ± 5.3) serotypes provided similar transduction efficiency and AAV2/2 transduced just 6% (± 2.6) of cells (**Fig. 1h;** $p<0.001$, ANOVA; n=3 independent differentiation cultures and **Fig. S1a,b**). Furthermore, ShH10.CMV.GFP^+ labeled cells were not only more numerous, but also had a stronger and brighter GFP expression (**Fig. S1c** for normalized MFI (median fluorescence intensity) fold-values). Using a high vector titre can be toxic to target cells[38] and thus it is also important to establish cell viability following transduction. To do this, we quantified by flow cytometry the percentage of early and late apoptotic (Live $dead^-$/$AnnexinV^+$ and Live $dead^+$/$AnnexinV^+$, respectively), necrotic (Live $dead^+$/$AnnexinV^-$) and live cells (Live $dead^-$/$AnnexinV^-$) in cultures transduced with each of the different vectors. No significant differences in cell viability were noted, regardless of the serotype used (**Fig. S1d**).

Targeting photoreceptor cells with AAV vectors is of particular interest as these cells contain the primary defect in the majority of retinal degenerations. We therefore investigated the ability of the six serotypes to transduce mESC-derived photoreceptors specifically. We demonstrated previously that, similar to photoreceptors from the postnatal retina[39,40] mESC-derived photoreceptors express a CD73 surface marker[41]. The percentage of CD73+ photoreceptor cells did not vary significantly between the different transduced cultures (**Fig. 1i**). However, the number of CD73+/CMV.GFP+ photoreceptor cells was significantly greater when cells were transduced with the ShH10 (24% ± 10.5%), compared with any of the other five serotypes (**Fig. 1i** ANOVA**,** $p < 0.0001$; n=3 independent differentiations **and Fig. S2a-c**). Furthermore, no significant difference in the number of viable CMV.GFP+/CD73+ photoreceptors was detected between any of the six serotypes (**Fig. S2d**).

ShH10 has been previously reported to specifically target astrocytes and Müller Glia following intravitreal (IV) injections[42]. We performed IV injections of the six CMV.GFP viruses into wild-type post-natal day 6 (P6) pups, a similar stage to days 22-24 of differentiation, to assess the potential of these viruses to transduce different cell types in the postnatal neural retina (**Fig. S3**). Similar to previous studies[42], we found that ShH10.CMV.GFP specifically transduces astrocytes and Müller glia following IV injections *in vivo* (**Fig. S3f**). However, immunohistochemistry analysis of ESC-derived wEBs transduced with ShH10.CMV.GFP demonstrated that neuroepithelium regions contained not only CRALBP+/GFP+ Müller glia cells but also many Recoverin+/GFP+ photoreceptors (**Fig. S4**). This is most likely due to increased viral vector accessibility *in vitro*. In the 3D wEB cultures, the presumptive inner nuclear layer (INL) is thinner, when compared with the postnatal retina, and these structures may lack astrocytes and the inner limiting membrane (ILM), both present at the vitreal surface of the postnatal retina. Our results demonstrate that ShH10 vectors are able to mediate significantly improved transduction

of mouse ESC-derived cells, including photoreceptors, compared with the other serotypes tested.

AAV transduction of mouse ESC-derived rods and cones using cell-specific promoters

To address questions of retinal and photoreceptor development using mouse ESC derived-retinal organoids it is often necessary to target rod and/or cone photoreceptor cells specifically. To determine the transduction efficiency of rods and cones *in vitro,* we used either a bovine Rhodopsin promoter[43] to obtain rod-specific expression or a human L-opsin cone promoter (PR2.1opsin.GFP)[44] to obtain cone-specific expression. We compared the transduction efficiency of an AAV2/9 vector with ShH10. Both AAV2/9.Rhop.GFP and ShH10.Rhop.GFP robustly and specifically labelled rod photoreceptors in 3D cultures, as demonstrated by GFP co-localisation with the rod-specific protein Rhodopsin (**Fig. 2a**). In our mouse 3D retinal organoid cultures we do not observe M/L opsin positive cones[31]. However, subretinal injection of AAV2/8.PR2.1opsin.GFP virus into the mouse adult WT retina results in labeling of S cones, as well as M/L cones (**Fig. S5**). We therefore examined the efficiency of AAV2/9 and ShH10.PR2.1opsin.GFP transduction of S cones by co-localisation with S-opsin (blue opsin) (**Fig. 2b**). In wEBs transduced with either vector, GFP fluorescence co-localised with S-opsin staining. The percentage of Rhop.GFP+ rods and PR2.1opsin.GFP+ cones was significantly higher in wEBs transduced with ShH10 (24% ± 6.8 and 7% ± 1.3, respectively), compared with AAV2/9 (17% ± 5.0 and 4% ± 1.0, respectively) (**Fig. 2c and Fig. S6;** Unpaired t-test; rods $p< 0.05$, n=9; cones $p< 0.01$, n=4 independent differentiations). No significant differences in viability were detected between any of the vectors tested (**Fig. 2d**).

AAV transduction of mouse ESC-derived RPE

To investigate the tropism of AAV serotypes with respect to mESC-derived RPE. We used a 3D suspension differentiation protocol where the Wnt agonist BIO was added from day 5 of culture.

A schematic of RPE differentiation is shown in **Fig. 3a**. Using this method, neuroepithelia that under non-BIO control conditions[20] would normally generate thick neuroepithelium of retinal origin and a small number of pigmented RPE cells (**Fig. 3b**, black and white arrows, respectively), instead differentiate exclusively into thin, convoluted RPE layers (**Fig. 3b**, white arrows). First, we analysed the ability of the six AAV serotypes to transduce RPE derived from BIO-treated wEBs cultured in suspension. Sections of BIO-treated wEBs, positive for the early RPE marker Mitf, demonstrated the presence of CMV.GFP+ pigmented cells in all six serotypes tested (**Fig. 3c**). To quantify the proportion of RPE cells transduced, RPE regions were manually dissected from BIO-treated wEBs at day 14 of culture and plated to form adherent RPE monolayers that were positive for actin-label phalloidin and demonstrated the typical cobblestone-like RPE cell morphology (**Fig. 3d**). RPE monolayers were then transduced and the percentage of GFP+ RPE cells was quantified by manual cell counting. ShH10 and AAV2/5 achieved similar levels of transduction, with around 70% of RPE cells being GFP+ (71% ± 11.2 and 71% ± 26, respectively). These two serotypes were significantly more efficient at transducing mESC-derived RPE compared with the other 4 serotypes tested (**Fig. 3e;** $p<0.001$, ANOVA; n=3 independent differentiations).

AAV transduction of human PSC-retinal cells

AAV transduction of human PSC-derived RPE

Pluripotent stem cells provide a renewable source of human RPE cells that can be used to study normal and disease mechanisms *in vitro*. Patient-derived iPSC-derived RPE cells offer a disease modelling platform that may allow the development of new treatments. Here, to assess which AAV serotypes most efficiently transduce human pluripotent stem cell (hPSC)-derived RPE *in vitro,* we differentiated human ES and iPS cells into RPE using a previously described protocol[19,36]. A schematic of the differentiation and virus infection protocol is shown in **Figure 4a**.

Titre-matched vectors were added between days 50-60 of culture and the number of GFP+ RPE cells was quantified as before, 7 days following addition of vector. Similar to mouse ESC-derived RPE, hPSC-derived RPE cultures formed typical pigmented and polygonal adherent cultures that expressed phalloidin (**Fig. 4b**). All serotypes were able to transduce adherent cultures of hPSC-derived RPE *in vitro,* albeit with different efficiencies. The proportion of ShH10 CMV.GFP-transduced hPSC-derived RPE (76% ± 30) was significantly greater than for AAV2/9 (6% ± 3), AAV2/8 (6% ± 6), AAV2/8T (3% ± 2) and AAV2/2 (11% ± 6), but not compared with AAV2/5 (37%± 18) (**Fig. 4c;** $p < 0.01$, ANOVA; n=3 independent differentiations). Usually, hPSC-derived RPE fields are picked manually from a heterogeneous population of retinal cells and as a result the final population is not always composed entirely of RPE cells. Therefore, to ensure specific targeting of RPE cells *in vitro,* specific promoters are needed. We have previously described that an optimised RPE65 human promoter can drive GFP expression in hPSC-derived RPE cells[45]. Here, we assessed if the same was true for the well-described human vitelliform macular dystrophy 2 (VMD2) promoter. We found that this promoter can also be used to target RPE *in vitro* and the percentage of GFP+ RPE cells transduced with the ShH10.VMD2.GFP (79% ± 5%) was not significantly different from cells transduced with ShH10.CMV.GFP (92% ± 8%) (**Fig. 4d;** ANOVA; n=3 independent differentiations). Furthermore, despite greater levels of GFP expression present in RPE cells transduced with vector containing a CMV promoter than in cells transduced with vector containing the RPE-specific VMD2 promoter, no differences in the viability of the cells were observed (**Fig. 4e**). Our results demonstrate that AAV vectors can readily transduce human RPE cells *in vitro*, with ShH10 and AAV2/5 performing significantly better than other commonly used serotypes.

AAV transduction of human ESC-derived retinal organoids and photoreceptors

A number of protocols have been reported for the differentiation of hPSCs into retinal tissues and cell types. We have adapted previously described protocols[24,46] to generate retinal

neuroepithelia containing a layered neuroretina, including photoreceptors that exhibit rudimentary outer segments and synaptic structures[25]. A schematic of photoreceptor differentiation and virus infection protocol is shown in **Fig. 5a**. Briefly, human ESCs were kept in maintenance conditions to confluence, before adding FGF negative medium. Islands of pigmented RPE were observed 3-4 weeks later and continuous retinal neuroepithelium vesicles surrounded by RPE were observed from 4-7 weeks of culture. These retinal vesicles were then excised from the 2D cultures and cultured further in suspension. We sought to establish the most efficient AAV serotype to transduce hESC-derived photoreceptors *in vitro* by testing the same six vectors described above. Titre matched CMV.GFP AAV vectors were added to hESC-derived organoids at 13 weeks of culture and analysed for the presence of GFP+ 2 weeks later. All six vectors were able to transduce hESC-derived retinal vesicles. A low magnification image of an AAV2/8.CMV.GFP transduced vesicle shows a number of GFP+ cells within the vesicle (**Fig. S7a,a'**). Strikingly, however, none of these appeared to be photoreceptors, as identified by co-staining for RECOVERIN-(**Fig. 5b-h;** n=3 independent experiments N>18 vesicles). This was the case for all six serotypes, including ShH10, which was able to transduce mouse mESC-derived photoreceptors with very high efficiency. However, when viral transduction was performed 4 weeks later (17 weeks) CMV.GFP+/ RECOVERIN+ photoreceptors were observed in the ONL–like region (**Fig. 5i-m**). In organoids transduced with ShH10.CMV.GFP, other retinal cells, possibly Müller glia, were also GFP+ (**Fig.5l**). Flow cytometric analysis of hESC-derived organoids demonstrated equivalent transduction using AAV2/2 and ShH10 (19% ± 3 and 21% ± 4, respectively), which were significantly greater than all the other vectors tested (**Fig. 5n**; 4% ± 3 AAV2/9, 4% ± 3 AAV2/8, 5.5% ± 3 AAV2/8T, 4% ± 2.5% AAV2/5; $P < 0.001$, ANOVA; n=3 independent differentiations). Therefore, the transduction efficiency of human PSC-derived photoreceptors by AAV vectors appears to depend on the developmental stage of the host photoreceptor cells.

Testing promoter specificity in human ESC-derived photoreceptors

One requirement for many retinal gene therapy approaches is the specific targeting of photoreceptor cells that avoids off-target expression. There may also be a requirement to further discriminate between rod and cone photoreceptors. We therefore assessed the ability of our retinal organoid system to test the specificity of expression after AAV-mediated transduction of photoreceptor cells using cone- and rod-specific promoters. Titre-matched vectors containing the cone-specific PR2.1opsin promoter driving eGFP were added between weeks 13-14 of culture and retinal organoids were collected two weeks later for immunohistochemistry and flow cytometry. Despite the addition of vectors at early stages in culture (13 weeks) we observed a number of GFP+ cells displaying typical cone morphology, with large inner segments and presumptive synaptic pedicles (**Fig. 6a**). ShH10.PR2.1.GFP+ cells co-expressed the cone-specific protein, RXRγ, but not the rod photoreceptor-specific photopigment, RHODOPSIN (**Fig. 6b and c**, respectively), demonstrating that all the transduced cells were indeed cone photoreceptors. To establish the transduction efficiency of the different serotypes and promoter specificity for the different cone photoreceptors subtypes. We tested four different AAV serotypes (ShH10, AAV2/9, AAV2/5 and AAV2/8) in hESC-derived organoids. GFP+ cells were observed in all transduced hESC-derived organoids and, in keeping with their normal position in the human outer nuclear layer (ONL), positive cells were mostly observed at the apical edge of the neuroepithelium. The efficiency of the ShH10.PR2.1 vector (15% ± 5) was similar to AAV2/8.PR2.1 vector (13% ± 2), and was significantly greater than AAV2/9 (3% ± 1), AAV2/2 (2% ± 1) or AAV2/5 (2% ± 1) capsids (**Fig. 6d and Fig. S7;** $P < 0.001$, ANOVA; n=4 independent differentiations). To determine in which cone photoreceptor subtypes the PR2.1 promoter is active, we checked for co-localisation of GFP with red and green (L+M) opsins (M/L OPSIN) and blue opsin (S-OPSIN). Co-localisation of M-OPSIN and GFP+ cells was observed in the neuroepithelium (**Fig. 6e, arrow**). Co-localisation of GFP+ and S-OPSIN cones was also observed, but only in a small proportion of the S cones. These PR2.1opsin.GFP+/S-OPSIN+

cones were observed only in ShH10 and AAV2/8 transduced organoids, but not in AAV2/9, AAV2/2 and AAV2/5 transduced organoids (**Fig. 6f**, arrow). Next, to test if a previously described human Rhodopsin promoter[47] is active and drives expression of GFP in PSC-derived rod photoreceptors we used an ShH10 capsid (ShH10.hRho.GFP). Similar to serotypes bearing the CMV promoter, no GFP+ cells were observed following transduction at 13 weeks, but when administered at 17 weeks in culture, this vector readily transduced rod photoreceptors as observed by widespread GFP expression and co-localization with the rod specific marker, α-Rod Transducin (GNAT1) (**Fig. 6g, g'**). Finally, we also observed photoreceptor-specific labelling when using an ShH10 vector containing a human Rhodopsin Kinase promoter fragment[48] (ShH10.hRK.GFP). Despite the sporadic labelling at the time point tested (17 weeks), our results confirm that this promoter fragment is active in both ARRESTIN3+ human cone (**Fig. 6h, h'**) and GNAT1+ rod photoreceptors (**Fig. 6i,l'**) and is therefore an appropriate promoter for gene therapies targeting both types of photoreceptors.

The results presented here confirm that the PR2.1.opsin and hRhodopsin promoters mediate robust and specific expression in human cone and rod photoreceptors, respectively. The PR2.1 promoter is active predominantly in M/L-cones, but also in some blue S-cones when transduction efficiency is high. Again, the ShH10 capsid was the most efficient serotype for the transduction of human cone photoreceptors *in vitro*. Surprisingly, the AAV2/8 serotype, which transduced mouse ES-derived photoreceptors poorly, transduced human ESC-derived cones efficiently *in vitro*. Most importantly, our results demonstrate that cone photoreceptors can be transduced at early time points in culture, whilst GFP+ rod photoreceptors were only observed following transduction at later time points.

Discussion

Numerous studies have demonstrated successful gene supplementation to the RPE and photoreceptor cells via AAV vectors in animal models[49] and the translation of some of these findings into clinical trials has established the feasibility of AAV ocular gene therapy[5,6,50,51]. A number of parameters must be fulfilled by preclinical studies prior to starting a gene therapy clinical trial. These include establishing vector tropism, vector transduction efficiency, expression of the transgene specifically in the target cells, safety and finally rescue of a disease phenotype. These provide proof-of-concept, and are usually performed in mouse and larger animal models. In the last few years, with the advent of efficient gene editing techniques, there may also a requirement for additional pre-clinical proof-of-concept studies involving human retinal cells. Stem cell technology has evolved rapidly in the past decade and is now able to provide human retinal organoids for studying development and disease *in vitro* and for the development of therapeutic approaches involving gene editing. In order to facilitate the development of such therapies we compared the efficacy of various AAV viral vectors in mouse and human stem cell derived RPE and photoreceptor cells.

Much of our understanding about AAV tropism has been established in the mouse retina, together with larger animals including pigs and dogs. To our knowledge, this is the first time the efficiency of AAV serotypes have been compared in stem cell-derived mouse and human retinal cells. We report a marked difference in transduction efficiency, dependent upon the serotype used. Overall, the ShH10 serotype, an AAV6 variant generated by directed evolution methodology[42], performed superiorly compared with the other AAV serotypes tested. However, some serotypes performed similarly to ShH10, dependent on the cell type; AAV2/5 and AAV2/8 were equivalent to ShH10 at transducing mouse and human RPE, and human cone photoreceptors, respectively. Although very useful to selectively target Müller glia in mice via intravitreal injections, our studies demonstrate that this serotype can also be used *in vitro* to target mouse and human ESC-derived photoreceptors and RPE with high efficiency. Our

findings underline the importance of selecting the appropriate AAV serotype for efficient transduction of the target cells for *in vitro* studies.

Pluripotent stem cell-derived human retinal cells can also be used to test promoter specificity, which would otherwise be tested in non-human primates. Here we show that AAV vectors carrying GFP under the control of the CMV promoter drive robust expression in mouse ESC-derived photoreceptors. Interestingly, the same vectors failed to drive expression following administration to 13-week-old human ESC-derived photoreceptors, whereas transduction of 17-week-old neuroepithelia resulted in robust GFP expression in photoreceptors. This data is in agreement with recent reports demonstrating that the developmental stage of the retina influences AAV transduction efficiency in photoreceptor cells[7]. A recent study by Petit *et al.*, (2017) suggested that outer segments are necessary for viral transduction of rod photoreceptors[52]. Indeed, our data supports these findings, as 13-week-old neuroepithelia contains photoreceptor inner segments but not outer segments (OS)-like structures, while the first rudimentary OS structures are observed from 16 weeks of development[25]. In contrast, transduction of cones by vectors carrying PR2.1opsin.GFP was observed even in early stages of culture. This is also consistent with the study by Petit *et al*. which showed that cone, but not rod photoreceptors, were efficiently transduced at early post-natal stages in mice[52]. These results show that care should be taken when assessing vectors in retinal organoids, taking into account that the developmental stage of the organoid could potentially affect the transduction efficiency and expression levels. This explains why serotypes, such as AAV2/5 and 2/9, that are highly efficient in *in vivo* animal studies and mature retinal explants, do not appear to transduce a large proportion of rods in the retinal organoids.

While many animal studies have been performed to evaluate the specificity and efficiency of rod- and cone-specific promoters, there is little data regarding their efficacy in human photoreceptors. Here, we tested RPE-, cone- and rod-specific promoters in human ESC-derived retinal cultures. Although the use of human ESC-derived cells is valuable for establishing viral vector tropism for AAV gene therapy *in vitro* as well as promoter specificity, such *in vitro* cultures have their limitations and should not be used as a sole method to aid the choice of AAV vectors to be used in human trials. Similar caution should be applied when using *ex vivo* human retinal explants. Measurements of transduction efficiency and biodistribution need to be examined with caution, as these cultures cannot fully replicate the complex environment of the eye. The concentrated administration, and subsequent spread of viral particles within the confined environment of the subretinal space cannot be replicated readily *in vitro*. For this reason, such *in vitro* studies should be regarded as complementary to *in vivo* work using animal models for the evaluation of viral transduction. Furthermore, it is important to note that *in vitro* differentiation systems do not currently reach later stages of development, equivalent to the adult retina. Toxicity is another important issue that can only be assessed in animal models, as assessments of transgene toxicity in cultures are limited to the cellular level. Systemic toxicity regarding immune related reactions to viral vectors can only be studied *in vivo*.

In summary, we demonstrate the utility of PSC-derived retinal tissues as a test system for the development of gene therapy vectors. Furthermore, we have used this system to assess the tropism of six AAV serotypes for mouse and human photoreceptors and RPE cells and we demonstrate that PSC-derived cells can be used to test promoter specificity in human cells. A likely next step is the use of iPSC-derived retinal cells generated from patients with inherited retinopathies as *in vitro* models to test a variety of gene therapy strategies, including those involving gene editing.

Acknowledgments:

This work was supported by grants from the Medical Research Council UK (MR/J004553/1), European Research Council (ERC-2012-ADG_20120314), RP Fighting Blindness (GR576), Fight For Sight (1448/1449), the Macular Vision Research Foundation, The Miller's Trust, the Special Trustees of Moorfields Eye Charity and a generous donation by Mr Otto van der Wyck. A.G.C is a UCL Sensory systems and Therapies Fellow; D.G. is a Singapore A star PhD student; R.A.P. is a Royal Society University Research Fellow. R.R.A is partially funded by the Department of Health's National Institute for Health Research Biomedical Research Centre at Moorfields Eye Hospital. R.A.P is part-funded by Alcon Research Institute

Author Disclosure Statement: No competing financial interests exist.

References

1. Auricchio A, Smith AJ, Ali RR. The Future Looks Brighter After 25 Years of Retinal Gene Therapy. HUMAN GENE THERAPY. Mary Ann Liebert, Inc. 140 Huguenot Street, 3rd Floor New Rochelle, NY 10801 USA; 2017 Nov;28(11):982–7.

2. Bainbridge JWB, Smith AJ, Barker SS, et al. Effect of gene therapy on visual function in Leber's congenital amaurosis. N Engl J Med. Massachusetts Medical Society; 2008 May 22;358(21):2231–9.

3. Maguire AM, Simonelli F, Pierce EA, et al. Safety and efficacy of gene transfer for Leber's congenital amaurosis. N Engl J Med. Massachusetts Medical Society; 2008 May 22;358(21):2240–8.

4. Hauswirth WW, Aleman TS, Kaushal S, et al. Treatment of leber congenital amaurosis due to RPE65 mutations by ocular subretinal injection of adeno-associated virus gene vector: short-term results of a phase I trial. HUMAN GENE THERAPY. Mary Ann Liebert, Inc. 140 Huguenot Street, 3rd Floor New Rochelle, NY 10801 USA; 2008 Oct;19(10):979–90.

5. Jacobson SG, Cideciyan AV, Roman AJ, et al. Improvement and decline in vision with gene therapy in childhood blindness. N Engl J Med. Massachusetts Medical Society; 2015 May 14;372(20):1920–6.

6. Bainbridge JWB, Mehat MS, Sundaram V, et al. Long-Term Effect of Gene Therapy on Leber's Congenital Amaurosis. N Engk J Med. Massachusetts Medical Society; 2015 May 13;372(20):1887–97.

7. Watanabe S, Sanuki R, Ueno S, et al. Tropisms of AAV for Subretinal Delivery to the Neonatal Mouse Retina and Its Application for In Vivo Rescue of Developmental Photoreceptor Disorders. PLoS ONE. Public Library of Science; 2013 Jan 15;8(1):e54146.

8. Mowat FM, Gornik KR, Dinculescu A, et al. Tyrosine capsid-mutant AAV vectors for gene delivery to the canine retina from a subretinal or intravitreal approach. Gene Ther. Nature Publishing Group; 2014 Jan;21(1):96–105.

9. Annear MJ, Mowat FM, Bartoe JT, et al. Successful gene therapy in older Rpe65-deficient dogs following subretinal injection of an adeno-associated vector expressing RPE65. HUMAN GENE THERAPY. 2013 Oct;24(10):883–93.

10. Colella P, Trapani I, Cesi G, et al. Efficient gene delivery to the cone-enriched pig retina by dual AAV vectors. Gene Ther. 2014 Apr;21(4):450–6.

11. Manfredi A, Marrocco E, Puppo A, et al. Combined rod and cone transduction by adeno-associated virus 2/8. HUMAN GENE THERAPY. 2013 Dec;24(12):982–92.

12. Mussolino C, Corte della M, Rossi S, et al. AAV-mediated photoreceptor transduction of the pig cone-enriched retina. Gene Ther. Nature Publishing Group; 2011 Jul;18(7):637–45.

13. Ye G-J, Budzynski E, Sonnentag P, et al. Cone-Specific Promoters for Gene Therapy of Achromatopsia and Other Retinal Diseases. HUMAN GENE THERAPY. 2016 Jan;27(1):72–82.

14. Boye SE, Alexander JJ, Boye SL, et al. The human rhodopsin kinase promoter in an AAV5 vector confers rod- and cone-specific expression in the primate retina. HUMAN GENE THERAPY. 2012 Oct;23(10):1101–15.

15. Wiley LA, Burnight E, Kaalberg EE, et al. Assessment of aav serotype tropism in human retinal explants. HUMAN GENE THERAPY. 2017 Nov 21;: hum.2017.179.

16. De Silva SR, Charbel Issa P, Singh MS, et al. Single residue AAV capsid mutation improves transduction of photoreceptors in the Abca4-/- mouse and bipolar cells in the rd1 mouse and human retina ex vivo. Gene Ther. Nature Publishing Group; 2016 Nov;23(11):767–74.

17. Orlans HO, Edwards TL, De Silva SR, et al. Human Retinal Explant Culture for Ex Vivo Validation of AAV Gene Therapy. Methods Mol Biol. New York, NY: Springer New York; 2018;1715(Chapter 21):289–303.

18. Osakada F, Ikeda H, Mandai M, et al. Toward the generation of rod and cone photoreceptors from mouse, monkey and human embryonic stem cells. Nat Biotechnol.

2008 Feb 3;26(2):215–24.

19. Meyer JS, Shearer RL, Capowski EE, et al. Modeling early retinal development with human embryonic and induced pluripotent stem cells. PNAS. 2009 Sep 29;106(39):16698–703.

20. Eiraku M, Takata N, Ishibashi H, et al. Self-organizing optic-cup morphogenesis in three-dimensional culture. Nature. Nature Publishing Group; 2011 Mar 29;472(7341):51–6.

21. Phillips MJ, Wallace KA, Dickerson SJ, et al. Blood-derived human iPS cells generate optic vesicle-like structures with the capacity to form retinal laminae and develop synapses. Investigative Ophthalmology & Visual Science. 2012 Apr;53(4):2007–19.

22. Nakano T, Ando S, Takata N, et al. Self-Formation of Optic Cups and Storable Stratified Neural Retina from Human ESCs. Cell stem cell. 2012 Jun 14;10(6):771–85.

23. Mellough CB, Sernagor E, Moreno-Gimeno I, et al. Efficient stage-specific differentiation of human pluripotent stem cells toward retinal photoreceptor cells. Stem Cells. 2012 Apr;30(4):673–86.

24. Zhong X, Gutierrez C, Xue T, et al. Generation of three-dimensional retinal tissue with functional photoreceptors from human iPSCs. Nat Commun. 2014;5:4047.

25. Gonzalez Cordero A, Kruczek K, Naeem A, et al. Recapitulation of Human Retinal Development from Human Pluripotent Stem Cells Generates Transplantable Populations of Cone Photoreceptors. Stem Cell Reports. 2017 Sep 12;9(3):820–37.

26. Li Y, Wu W-H, Hsu C-W, et al. Gene therapy in patient-specific stem cell lines and mice with membrane frizzled-related protein (MFRP) defects. Molecular Therapy. 2014 Jun 4.

27. Singh R, Shen W, Kuai D, et al. iPS cell modeling of Best disease: insights into the pathophysiology of an inherited macular degeneration. Human Molecular Genetics. 2013 Jan 11;22(3):593–607.

28. Phillips MJ, Perez ET, Martin JM, et al. Modeling human retinal development with patient-specific induced pluripotent stem cells reveals multiple roles for visual system homeobox 2. Stem Cells. 2014 Jun;32(6):1480–92.

29. Jin Z-B, Okamoto S, Osakada F, et al. Modeling retinal degeneration using patient-specific induced pluripotent stem cells. Mattson M, editor. PLoS ONE. 2011 Feb 10;6(2):e17084.

30. Gonzalez Cordero A, West EL, Pearson RA, et al. Photoreceptor precursors derived from three-dimensional embryonic stem cell cultures integrate and mature within adult degenerate retina. Nat Biotechnol. 2013 Aug;31(8):741–7.

31. Kruczek K, Gonzalez Cordero A, Goh D, et al. Differentiation and Transplantation of Embryonic Stem Cell-Derived Cone Photoreceptors into a Mouse Model of End-Stage Retinal Degeneration. Stem Cell Reports. 2017 Jun 6;8(6):1659–74.

32. Ovando-Roche P, Georgiadis A, Smith AJ, et al. Harnessing the Potential of Human Pluripotent Stem Cells and Gene Editing for the Treatment of Retinal Degeneration. Curr Stem Cell Rep. Springer International Publishing; 2017;3(2):112–23.

33. Kim H, Kim J-S. A guide to genome engineering with programmable nucleases. Nat Rev Genet. Nature Publishing Group; 2014 May;15(5):321–34.

34. Peddle CF, Maclaren RE. The Application of CRISPR/Cas9 for the Treatment of Retinal Diseases. Yale J Biol Med. Yale Journal of Biology and Medicine; 2017 Dec;90(4):533–

41.

35. West EL, Gonzalez Cordero A, Hippert C, et al. Defining the integration capacity of embryonic stem cell-derived photoreceptor precursors. Stem Cells. 2012 Jul;30(7):1424–35.

36. Meyer JS, Howden SE, Wallace KA, et al. Optic vesicle-like structures derived from human pluripotent stem cells facilitate a customized approach to retinal disease treatment. Stem Cells. 2011 Aug;29(8):1206–18.

37. Nishiguchi KM, Carvalho LS, Rizzi M, et al. Gene therapy restores vision in rd1 mice after removal of a confounding mutation in Gpr179. Nat Commun. Nature Publishing Group; 2015 Jan 23;6:6006.

38. Howard DB, Powers K, Wang Y, et al. Tropism and toxicity of adeno-associated viral vector serotypes 1, 2, 5, 6, 7, 8, and 9 in rat neurons and glia in vitro. Virology. 2008 Mar 1;372(1):24–34.

39. Lakowski J, Han YT, Pearson RA, et al. Effective Transplantation of Photoreceptor Precursor Cells Selected Via Cell Surface Antigen Expression. Stem Cells. 2011;29(9):1391–404.

40. Eberle D, Schubert S, Postel K, et al. Increased integration of transplanted CD73-positive photoreceptor precursors into adult mouse retina. Investigative Ophthalmology & Visual Science. 2011 Aug;52(9):6462–71.

41. Lakowski J, Gonzalez Cordero A, West EL, et al. Transplantation of Photoreceptor Precursors Isolated via a Cell Surface Biomarker Panel From Embryonic Stem Cell-Derived Self-Forming Retina. Stem Cells. 2015 Aug;33(8):2469–82.

42. Klimczak RR, Koerber JT, Dalkara D, et al. A novel adeno-associated viral variant for efficient and selective intravitreal transduction of rat Müller cells. Fugmann SD, editor. PLoS ONE. Public Library of Science; 2009 Oct 14;4(10):e7467.

43. Ali RR, Sarra GM, Stephens C, et al. Restoration of photoreceptor ultrastructure and function in retinal degeneration slow mice by gene therapy. Nat Genet. 2000 Jul;25(3):306–10.

44. Wang Y, Macke JP, Merbs SL, et al. A locus control region adjacent to the human red and green visual pigment genes. Neuron. 1992 Sep;9(3):429–40.

45. Georgiadis A, Duran Y, Ribeiro J, et al. Development of an optimized AAV2/5 gene therapy vector for Leber congenital amaurosis owing to defects in RPE65. Gene Ther. 2016 Dec;23(12):857–62.

46. Reichman S, Terray A, Slembrouck A, et al. From confluent human iPS cells to self-forming neural retina and retinal pigmented epithelium. pnasorg.

47. Zack DJ, Bennett J, Wang Y, et al. Unusual topography of bovine rhodopsin promoter-lacZ fusion gene expression in transgenic mouse retinas. Neuron. Cell Press; 1991 Feb 1;6(2):187–99.

48. Khani SC, Pawlyk BS, Bulgakov OV, et al. AAV-Mediated Expression Targeting of Rod and Cone Photoreceptors with a Human Rhodopsin Kinase Promoter. Investigative Ophthalmology & Visual Science. 2007 Sep 1;48(9):3954–61.

49. Smith AJ, Bainbridge JWB, Ali RR. Gene supplementation therapy for recessive forms of inherited retinal dystrophies. Gene Ther. Nature Publishing Group; 2012 Feb;19(2):154–61.

50. Weleber RG, Pennesi ME, Wilson DJ, et al. Results at 2 Years after Gene Therapy for RPE65-Deficient Leber Congenital Amaurosis and Severe Early-Childhood-Onset Retinal Dystrophy. Ophthalmology. 2016 Jul;123(7):1606–20.

51. Testa F, Maguire AM, Rossi S, et al. Three-year follow-up after unilateral subretinal delivery of adeno-associated virus in patients with Leber congenital Amaurosis type 2. Ophthalmology. 2013 Jun;120(6):1283–91.

52. Petit L, Ma S, Cheng S-Y, et al. Rod Outer Segment Development Influences AAV-Mediated Photoreceptor Transduction After Subretinal Injection. HUMAN GENE THERAPY. 2017 Jun;28(6):464–81.

Figure 1.

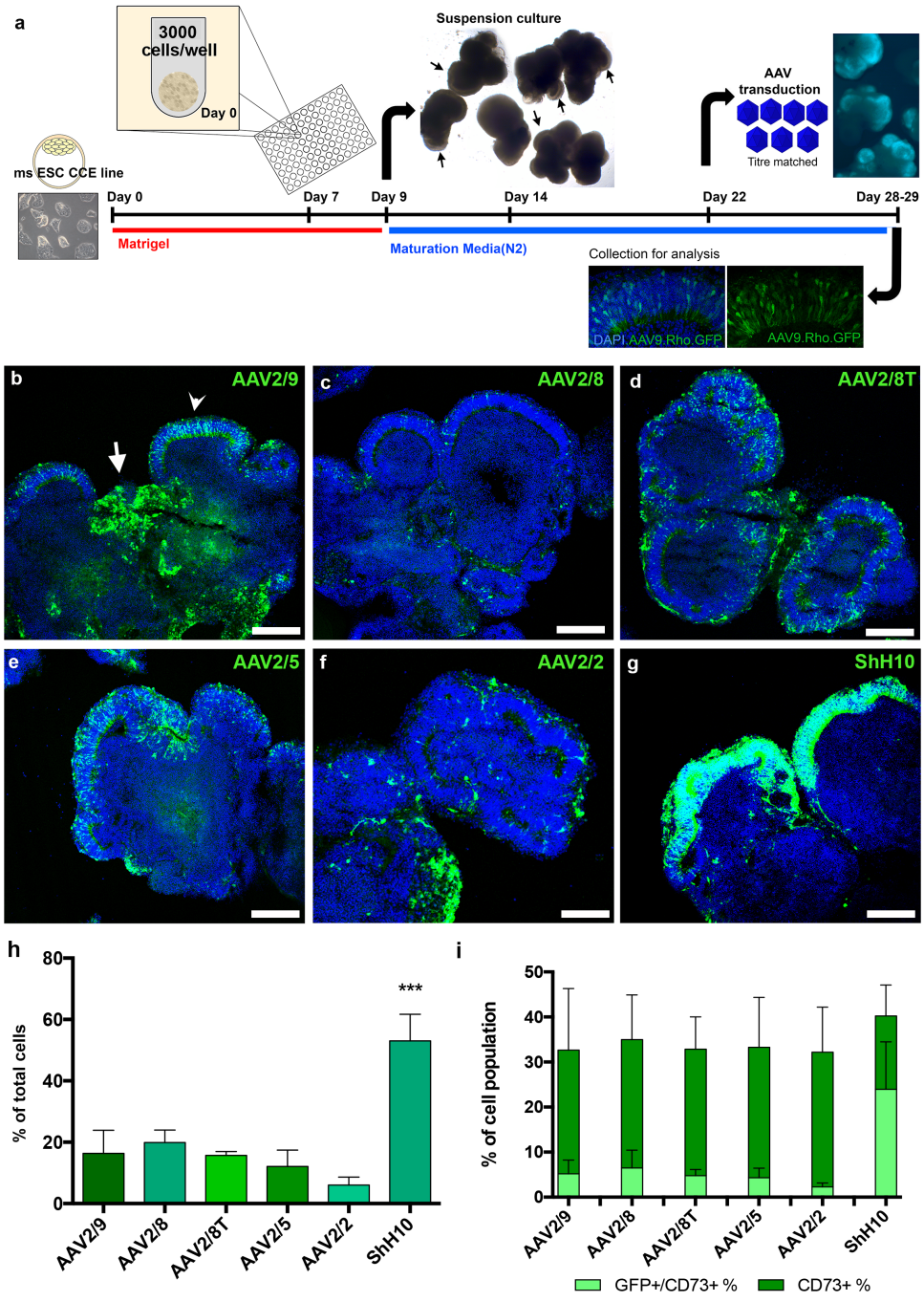
a
3000 cells/well
Day 0
ms ESC CCE line
Suspension culture
AAV transduction
Titre matched
Day 0
Day 7
Day 9
Day 14
Day 22
Day 28-29
Matrigel
Maturation Media(N2)
Collection for analysis
DAPI.AAV9.Rho.GFP
AAV9.Rho.GFP
b AAV2/9
c AAV2/8
d AAV2/8T
e AAV2/5
f AAV2/2
g ShH10
h
% of total cells
***
AAV2/9
AAV2/8
AAV2/8T
AAV2/5
AAV2/2
ShH10
i
% of cell population
GFP+/CD73+ %
CD73+ %

Figure 2.

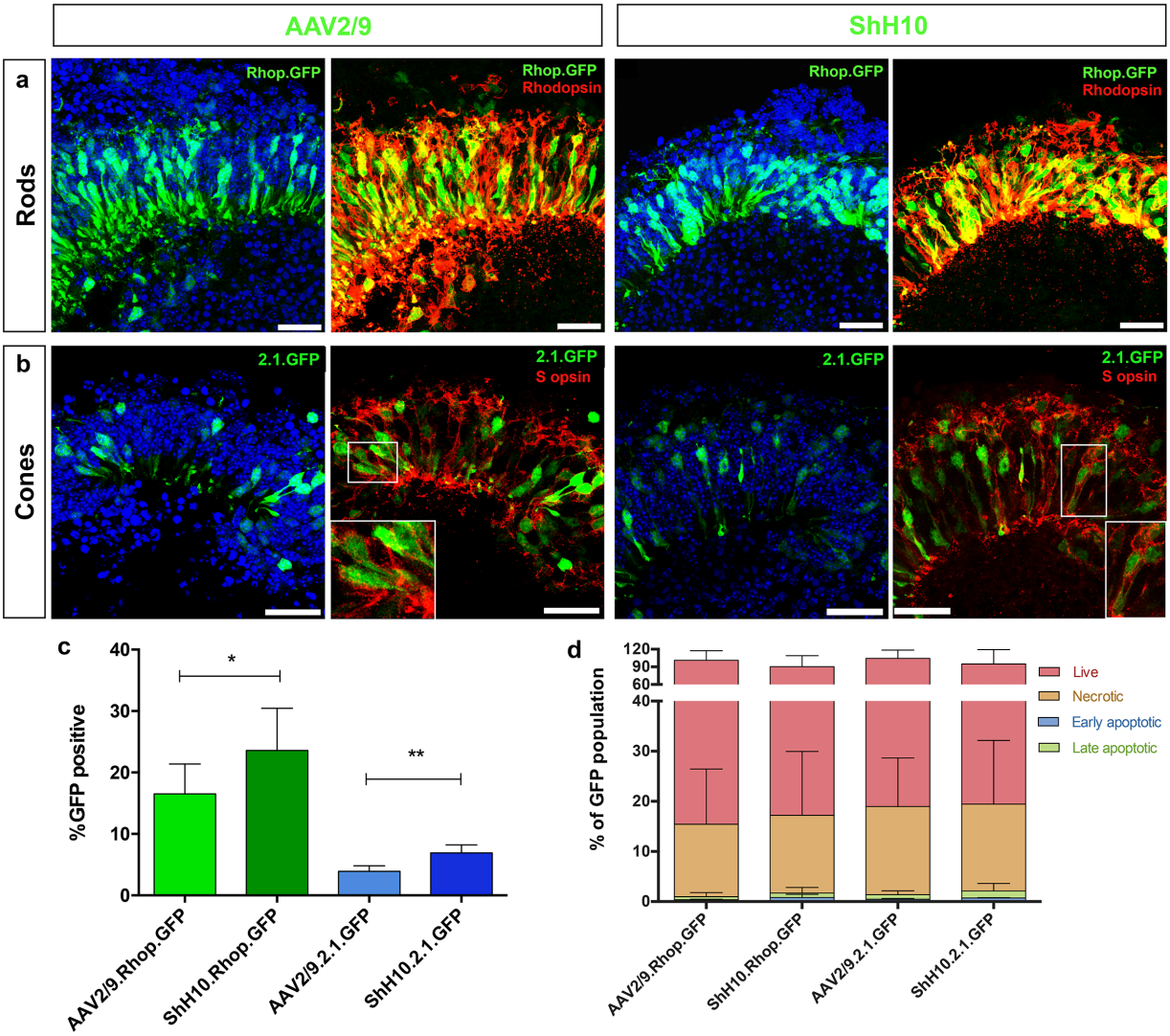
AAV2/9
ShH10
a
Rods
Rhop.GFP
Rhop.GFP
Rhodopsin
Rhop.GFP
Rhop.GFP
Rhodopsin
b
Cones
2.1.GFP
2.1.GFP
S opsin
2.1.GFP
2.1.GFP
S opsin
c
%GFP positive
40
30
20
10
0
*
**
AAV2/9.Rhop.GFP
ShH10.Rhop.GFP
AAV2/9.2.1.GFP
ShH10.2.1.GFP
d
% of GFP population
120
90
60
40
30
20
10
0
Live
Necrotic
Early apoptotic
Late apoptotic
AAV2/9.Rhop.GFP
ShH10.Rhop.GFP
AAV2/9.2.1.GFP
ShH10.2.1.GFP

Figure 3.

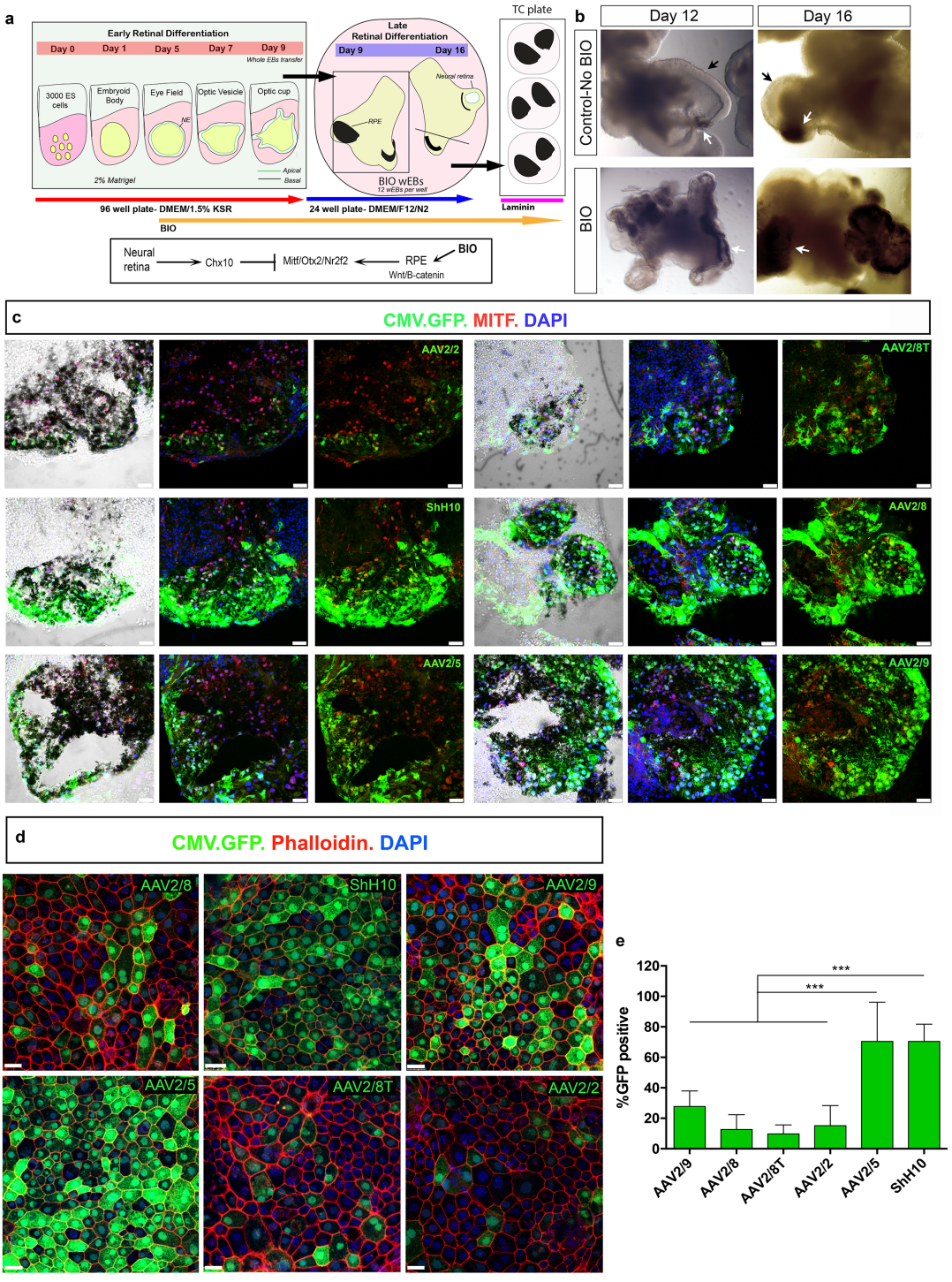
a
Early Retinal Differentiation
Day 0
Day 1
Day 5
Day 7
Day 9
Whole EBs transfer
3000 ES cells
Embryoid Body
Eye Field
Optic Vesicle
Optic cup
NE
2% Matrigel
Apical
Basal
Late Retinal Differentiation
Day 9
Day 16
Neural retina
RPE
BIO wEBs
12 wEBs per well
TC plate
Laminin
96 well plate- DMEM/1.5% KSR
24 well plate- DMEM/F12/N2
BIO
Neural retina
Chx10
Mitf/Otx2/Nr2f2
RPE
BIO
Wnt/B-catenin
b
Day 12
Day 16
Control-No BIO
BIO
c
CMV.GFP. MITF. DAPI
AAV2/2
AAV2/8T
ShH10
AAV2/8
AAV2/5
AAV2/9
d
CMV.GFP. Phalloidin. DAPI
AAV2/8
ShH10
AAV2/9
AAV2/5
AAV2/8T
AAV2/2
e
%GFP positive
120
100
80
60
40
20
0
***
***
AAV2/9
AAV2/8
AAV2/8T
AAV2/2
AAV2/5
ShH10

Figure 4.

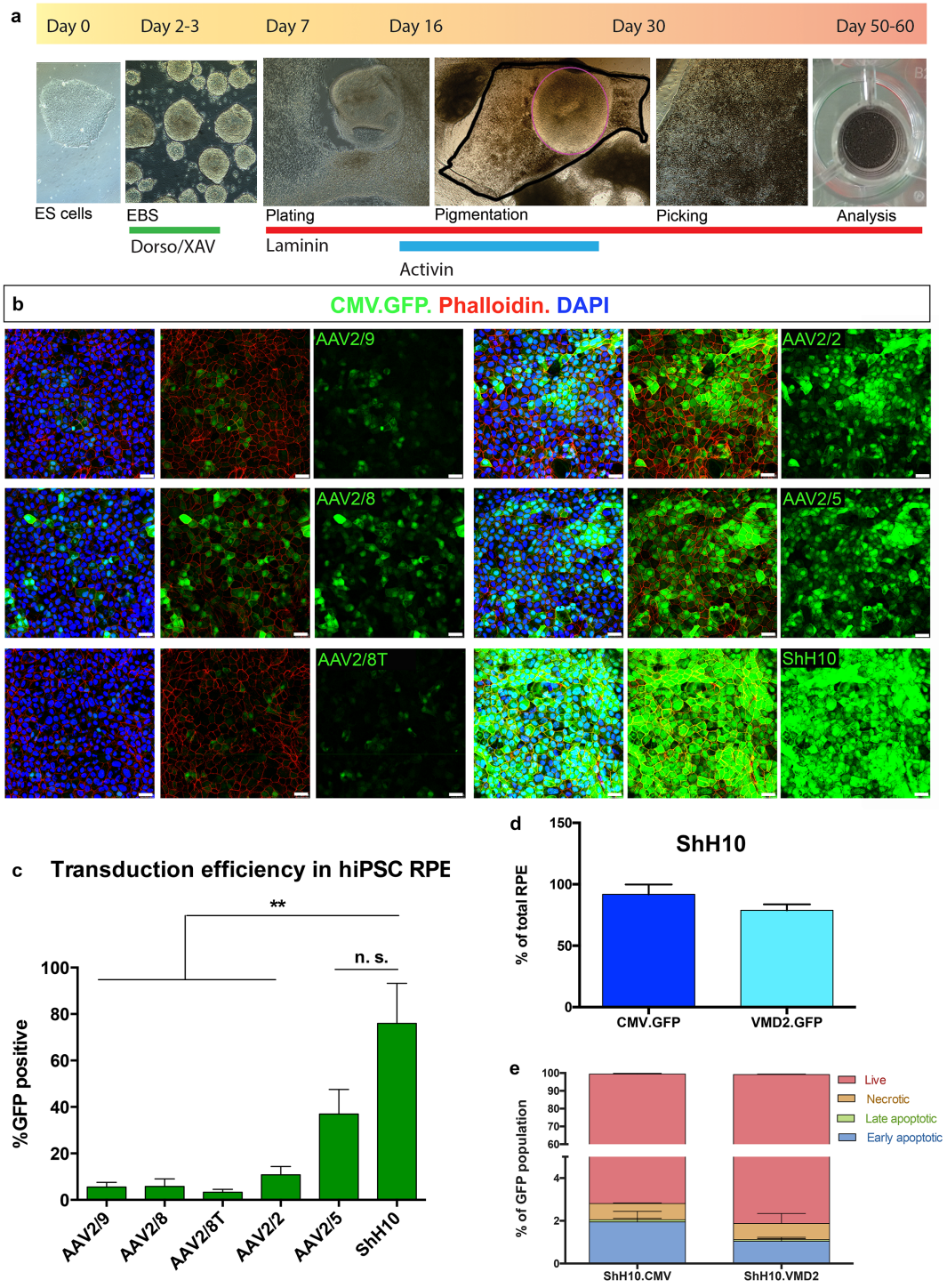
a
Day 0
Day 2-3
Day 7
Day 16
Day 30
Day 50-60
ES cells
EBS
Plating
Pigmentation
Picking
Analysis
Dorso/XAV
Laminin
Activin
b
CMV.GFP. Phalloidin. DAPI
AAV2/9
AAV2/2
AAV2/8
AAV2/5
AAV2/8T
ShH10
c
Transduction efficiency in hiPSC RPE
**
n. s.
%GFP positive
100
80
60
40
20
0
AAV2/9
AAV2/8
AAV2/8T
AAV2/2
AAV2/5
ShH10
d
ShH10
% of total RPE
150
100
50
0
CMV.GFP
VMD2.GFP
e
% of GFP population
100
90
80
70
60
4
2
0
Live
Necrotic
Late apoptotic
Early apoptotic
ShH10.CMV
ShH10.VMD2

Figure 5.

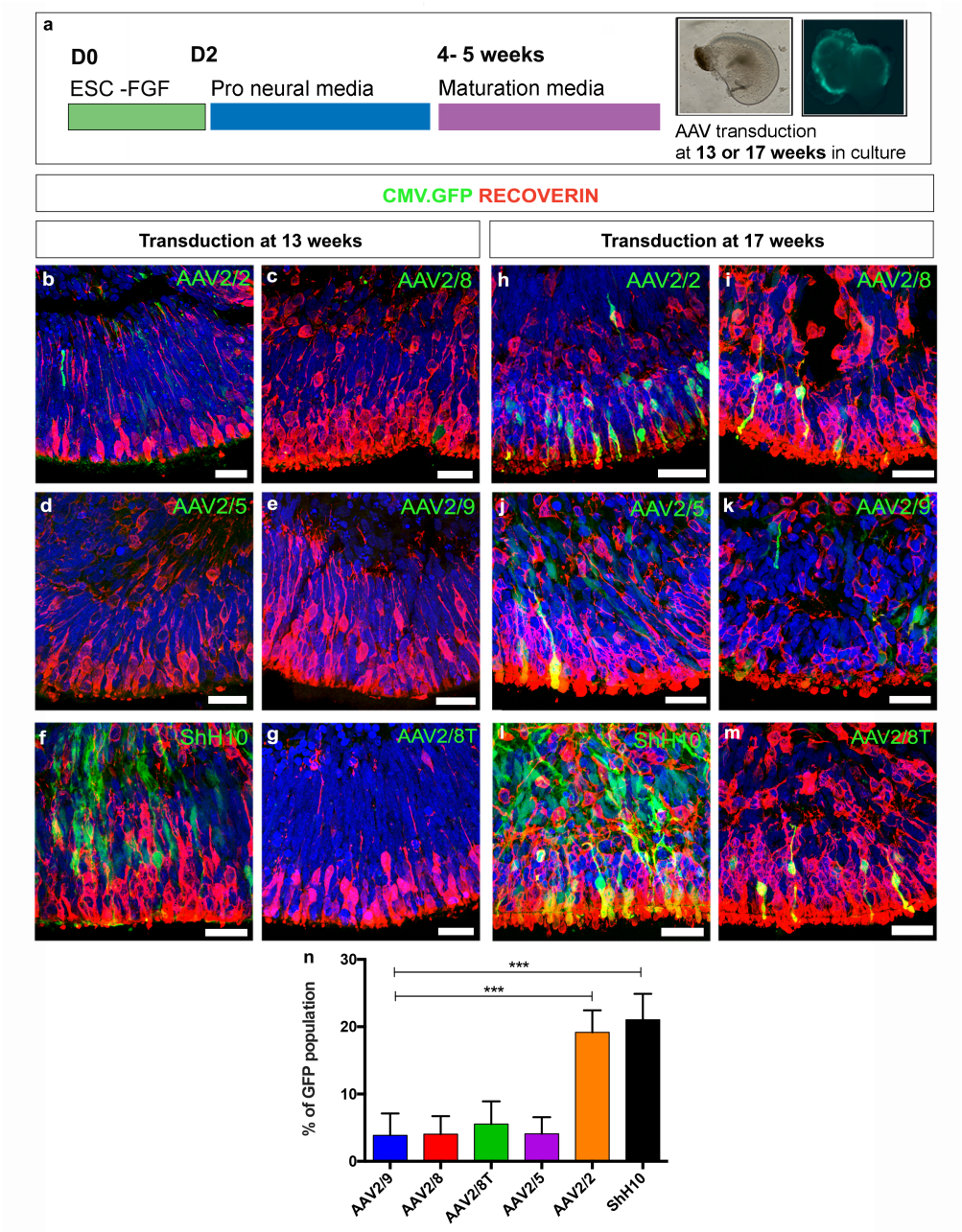
a
D0
D2
4- 5 weeks
ESC -FGF
Pro neural media
Maturation media
AAV transduction
at 13 or 17 weeks in culture
CMV.GFP RECOVERIN
Transduction at 13 weeks
Transduction at 17 weeks
b AAV2/2
c AAV2/8
h AAV2/2
i AAV2/8
d AAV2/5
e AAV2/9
j AAV2/5
k AAV2/9
f ShH10
g AAV2/8T
l ShH10
m AAV2/8T
n
% of GFP population
30
20
10
0
***
***
AAV2/9
AAV2/8
AAV2/8T
AAV2/5
AAV2/2
ShH10

Figure 6.

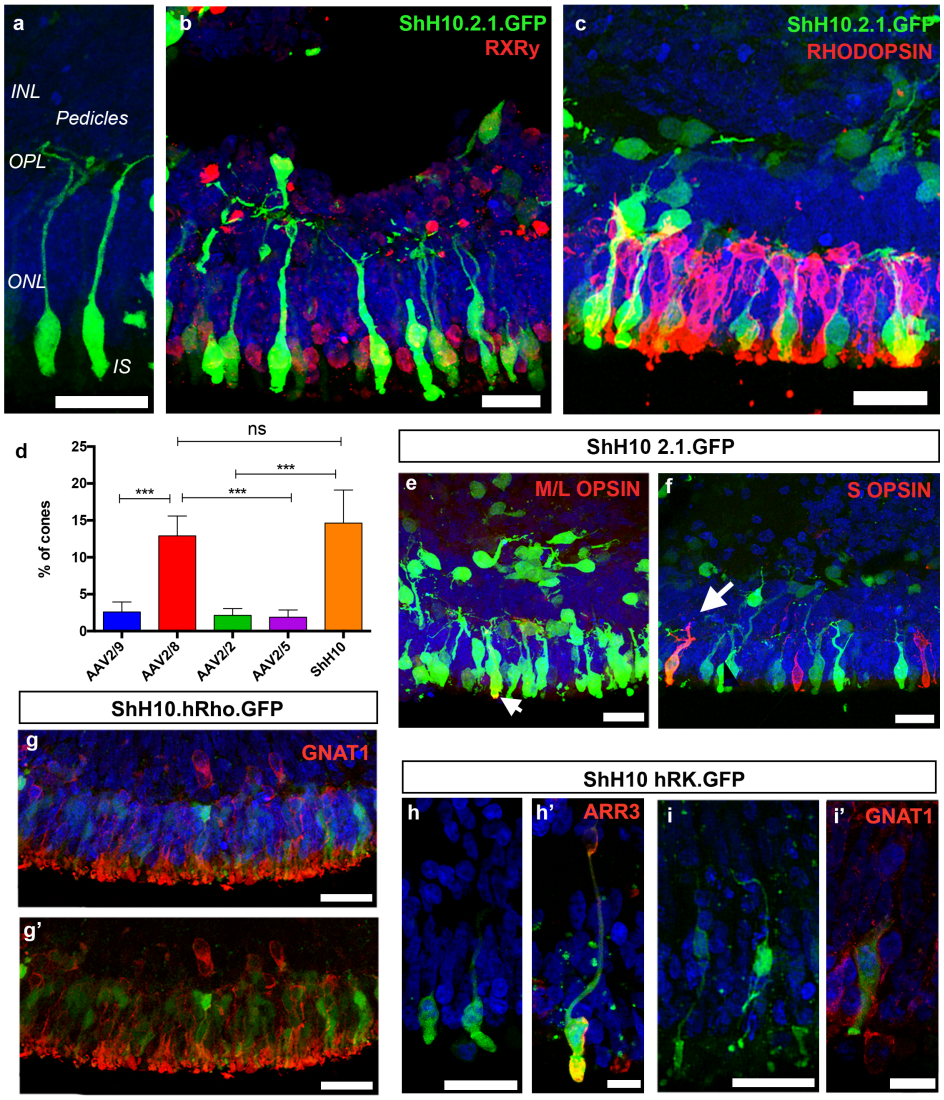

Figure Legends:

Figure 1. Establishing AAV tropism in mouse ESC-derived wEBs

a. Schematic showing mouse ESC differentiation protocol into photoreceptors and viral labelling strategy. **b-g.** Representative images of wEBs showing GFP expression (green) under the control of a CMV promoter for the six AAV serotypes tested. **h.** Quantification of the % of cells that is GFP positive after transduction in culture. **i.** Percentage of cells that are photoreceptors (CD73+) and the percentage of cells that are transduced photoreceptors (GFP+/CD73+) in cultures transduced by the six AAV serotypes tested. Nuclei were stained with DAPI (blue). Scale bars: 100 μm (**b-g**).

Figure 2. Testing promoter specificity in mouse ESC-derived photoreceptors

a. Images showing co-expression of Rhodopsin (red) and GFP driven by Rhodopsin promoter (green) after AAV2/9 and ShH10-mediated gene delivery. **b.** Images showing co-expression of Sopsin (red) and GFP driven by Mopsin (2.1PR) promoter (green). **c.** Percentage of GFP positive rods and cones transduced by AAV2/9 and ShH10 serotypes. D. Percentage of live, necrotic, late apoptotic and early apoptotic rod and cone photoreceptors following AAV2/9 and ShH10 transduction. Nuclei were stained with DAPI (blue). Scale bars: 25 μm (**a, b**).

Figure 3. Establishing AAV tropism in mouse ESC-derived RPE

a. Schematic showing BIO treatment for mESC-derived RPE differentiation. RPE regions from wEBs were dissected and plated on laminin-coated plates. **b.** Bright field images showing wEBs that have been though retinal and RPE differentiation. **c.** Representative images showing the pigmented RPE regions on wEBs that have been

transduced by the six CMV.GFP AAV serotypes. **d.** Images showing virally transduced RPE monolayer cultures stained with Phalloidin. **e.** Percentage of GFP+ mESC-derived RPE cells transduced by the six AAV serotypes tested. Nuclei were stained with DAPI (blue). Scale bars: 25 μm (**c,d**).

Figure 4. Establishing AAV tropism in human iPS-derived RPE

a. Schematic of human pluripotent stem cells differentiation into hiPS-derived RPE. **b.** Representative image showing virally transduced hiPS-derived RPE monolayer cultures stained for Phalloidin. **c.** Percentage of GFP+ hiPS-derived RPE cells transduced by the by the six AAV serotypes tested. **d.** Percentage of hiPS-derived RPE transduced by ShH10 carrying either a CMV or a VMD2 promoter. **e.** Percentage of live, necrotic, late apoptotic and early apoptotic rod and cone photoreceptors following ShH10 transduction. Nuclei were stained with DAPI (blue). Scale bars: 25 μm (**b**).

Figure 5. Establishing AAV tropism in human ESC-derived retinal organoids

a. Timeline schematic of human stem cell differentiation into hESC-derived photoreceptors and viral labelling. **b-m.** Representative high magnification images of neuroepithelial regions transduced by six AAV serotypes at 12 weeks (**b-g) and** 17 weeks (**h-m)** of development. No GFP+ photoreceptors were observed for any of the six vectors when transduced at 12 weeks, whilst GFP+ photoreceptors were present in late transduced cultures. **n.** Percentage of GFP+ cells in retinal organoids transduced at 17 weeks of culture. Nuclei were stained with DAPI (blue). Scale bars: 25 μm (**b-m**).

Figure 6. Testing promoter specificity in human ESC-derived photoreceptors

a. Image highlighting the morphology of ShH10.2.1.GFP transduced cells. **b.** ShH10.2.1.GFP cells co-localised with RXRγ+ cone photoreceptors (red). **c.** ShH10.2.1.GFP cells did not co-localise with RHODOPSIN+ rod photoreceptors (red). **d.** Percentage of GFP+ hESC-derived cone photoreceptors transduced by the AAV serotypes tested. **e.** M/LOPSIN+ cones (red, arrows) co-localised with 2.1.GFP+ cones. **f.** SOPSIN+ cones (red, arrows) only co-localised with few 2.1.GFP+ cones in the highly transduced ShH10. **g, g'.** Image of a neuroepithelia region showing co-localisation of GNAT1+ rod photoreceptors and ShH10.hRhod.GFP transduced cells. **h-i'.** Images of neuroepithelia regions transduced with ShH10.hRK.GFP vector. **h',i'.** Images of a ARRESTIN3+ ShH10.hRK.GFP cone and GNAT1+ rod photoreceptors. Nuclei were stained with DAPI (blue). Scale bars: 25 μm (**a-c, e-i**), 10 μm (**h', i'**).

Supplementary information:

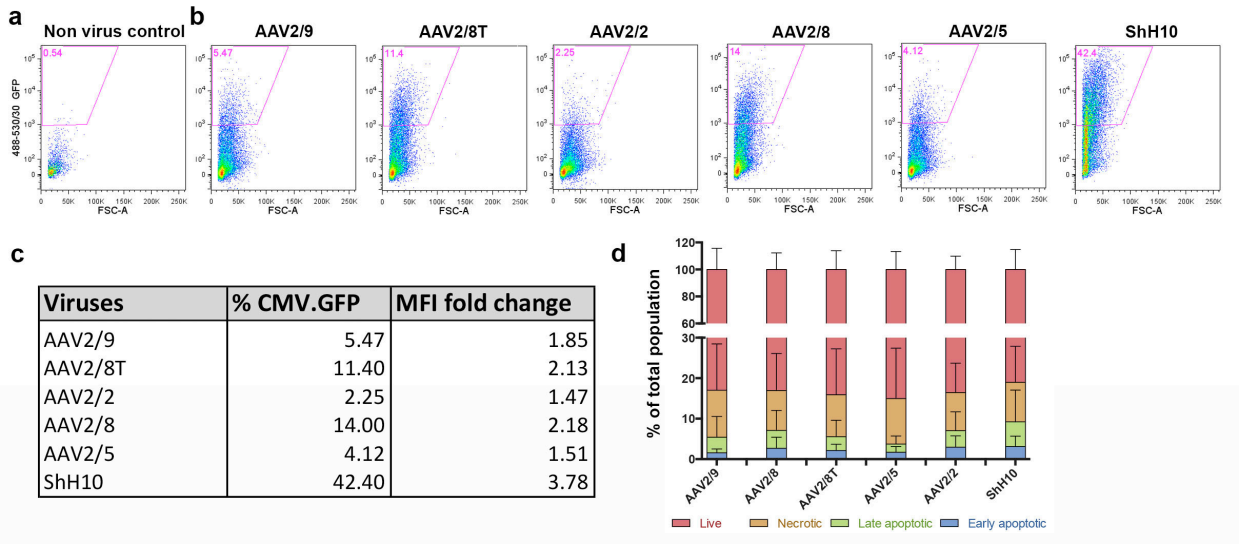

Viruses	% CMV.GFP	MFI fold change
AAV2/9	5.47	1.85
AAV2/8T	11.40	2.13
AAV2/2	2.25	1.47
AAV2/8	14.00	2.18
AAV2/5	4.12	1.51
ShH10	42.40	3.78

Supplementary Figure S1. Viral transduction efficiency of six AAV serotypes on mouse ESC-derived wEBs

Flow cytometry gate strategy for mouse ESC-derived wEB. **a.** Representative plot showing a negative control, non-virus transduced wEB, with GFP gate. **b.** Representative plots showing the percentage of GFP+ cells from each virus tested. **c.** Table showing the % GFP cells shown in c with corresponding MFI. **d.** Percentage of live, necrotic, late apoptotic and early apoptotic cells in the wEB population following virus transduction.

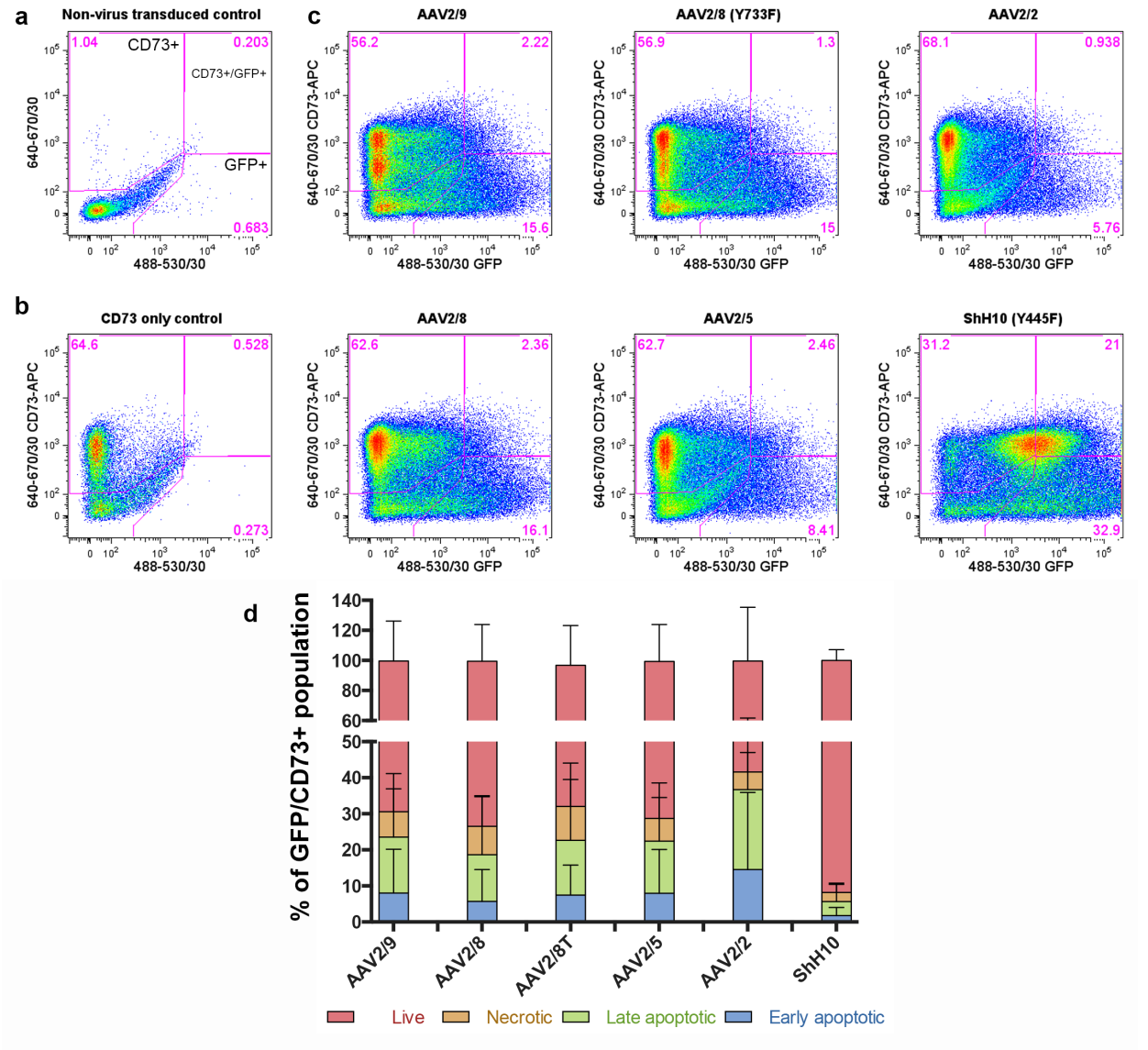

Supplementary Figure S2. Viral transduction efficiency of six AAV2 serotypes on mouse ESC-derived photoreceptors

Flow cytometry gate strategy of a mouse ESC-derived wEB. **a.** Representative plot of a non-virus transduced EB showing gates for GFP+ (bottom right panel), CD73+ (top left panel) and CD73+/GFP+ (top right panel). **b.** Representative plot of a non-virus transduced EB stained for photoreceptor marker CD73. **c.** Representative plots showing the percentage of GFP+ cells (bottom right panel), CD73+ photoreceptors and double positive CD73+/GFP+ photoreceptors for each virus tested. **d.** Percentage of live, necrotic, late apoptotic and early apoptotic CD73+/GFP+ photoreceptors.

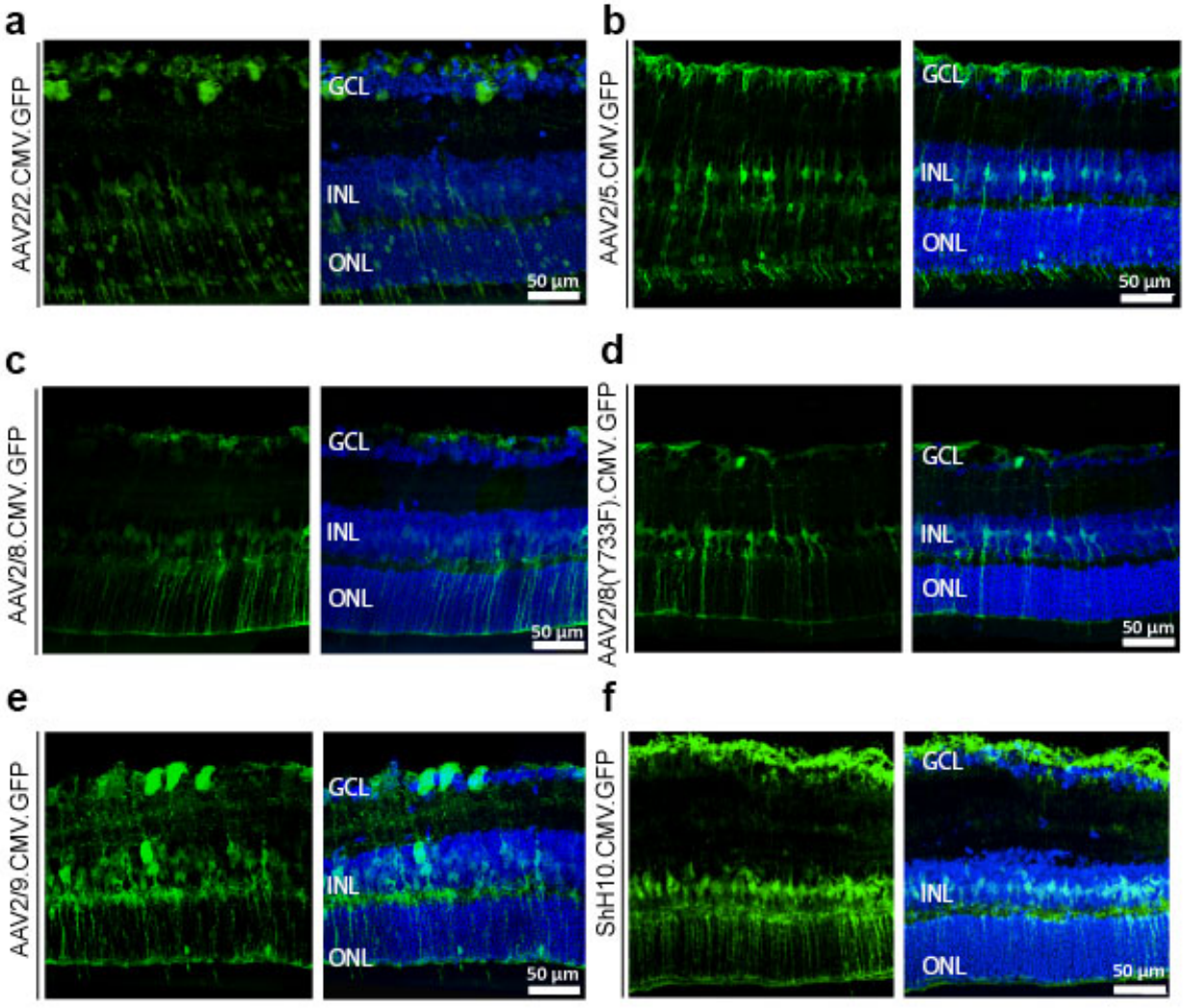

Supplementary Figure S3. Intravitreal injections of AAV vectors in wild type mice.

a-f. Images of young adult wild type retina intravitreally injected at P5.5-P6.5 with a range of AAV serotypes. Each AAV vector shows different transduction efficiency targeting interneurons in the INL. AAV2/2 and ShH10 showed widespread expression of GFP, with the later transducing mainly Muller glial cells.

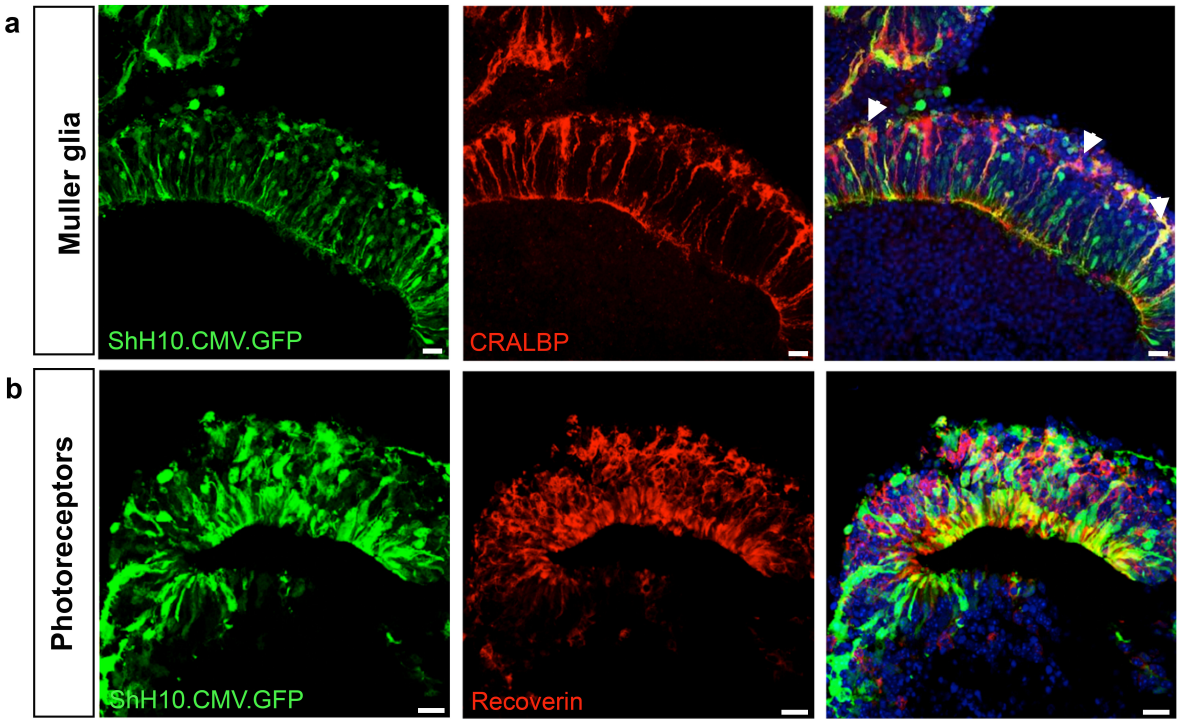

Supplementary Figure 4. Establishing ShH10 tropism in mouse ESC-derived cells

a. Image showing ShH10.CMV.GFP (green) transduced neuroepithelia region and co-localization with CRALBP+ (red) Muller cells. **b.** Image showing ShH10.CMV.GFP (green) transduced neuroepithelia region and co-localization with Recoverin+ (red) photoreceptor cells. Nuclei were stained with DAPI (blue). Scale bars: 25 μm.

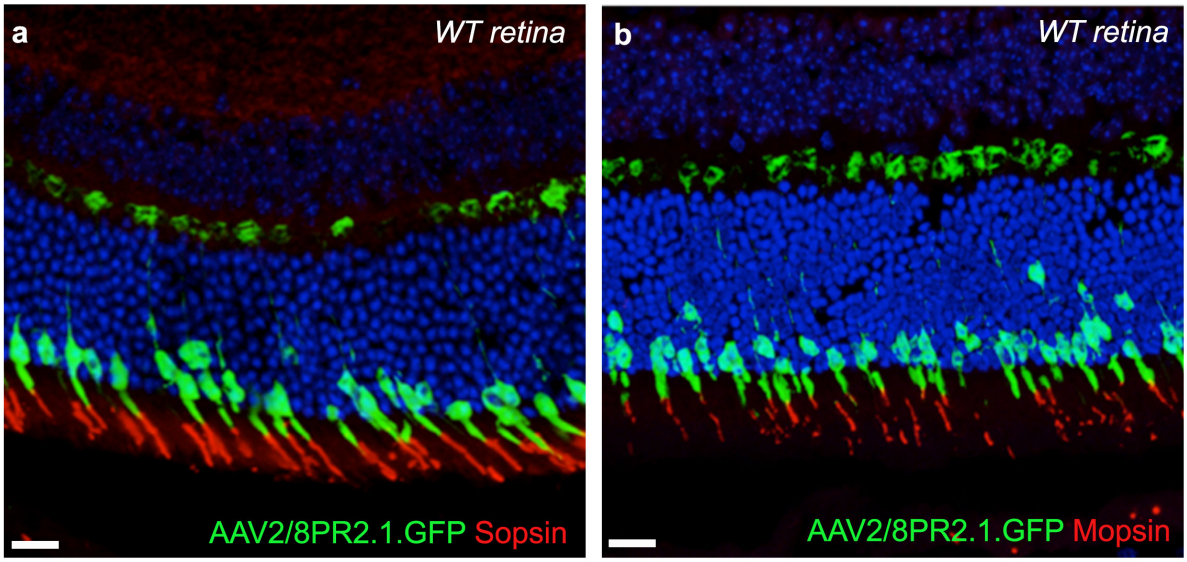

Supplementary Figure S5. Transduction specificity of AAV2/8.PR2.1.GFP in the adult wildtype retina

a. Image of a wild type retina subretinally injected with an AAV2/8.PR.2.1.GFP virus showing co-localisation of GFP with S-opsin cones (red). **b.** Image of the same wild type retina showing co-localisation of GFP with M-opsin cones (red). Nuclei were stained with DAPI (blue). Scale bars: 25μm (**a-b**).

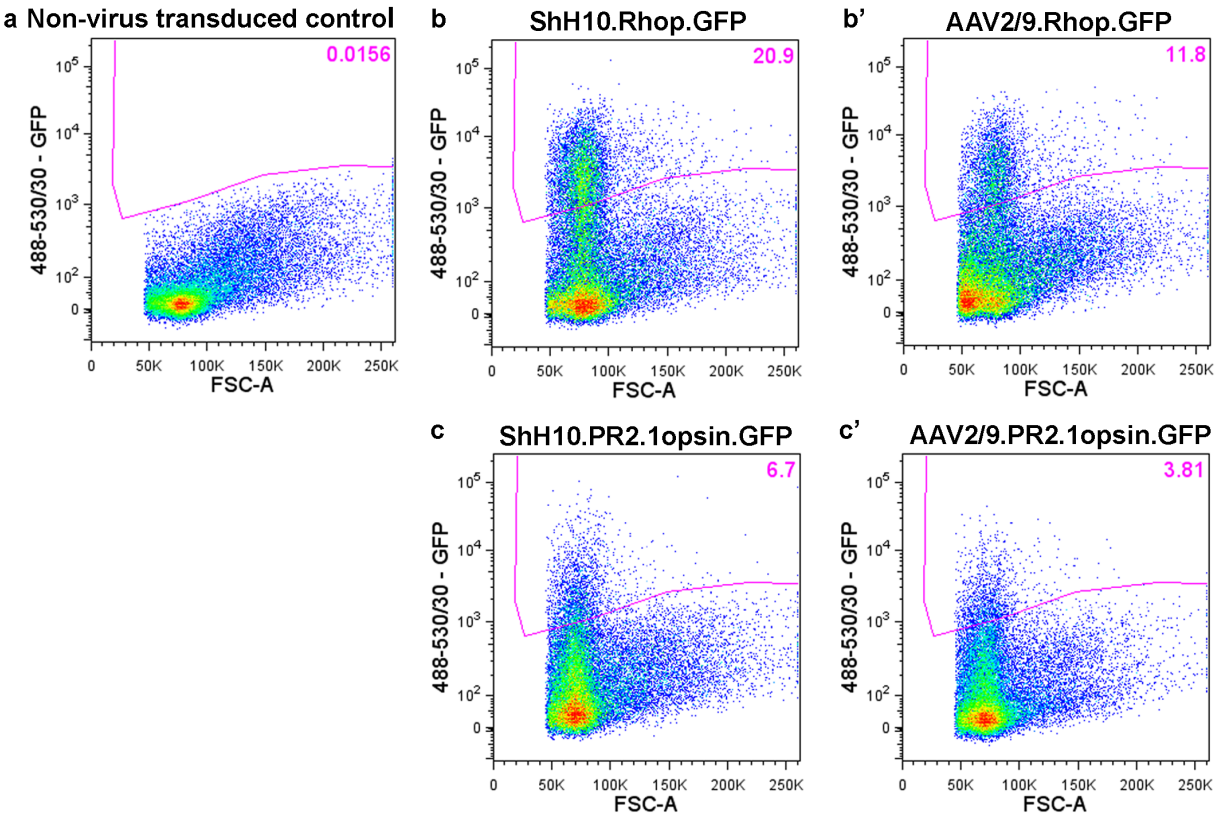

Supplementary Figure S6. Viral transduction efficiency of ShH10 and AAV2/9 serotypes on mouse ESC-derived rod and cone photoreceptors

Flow cytometry gate strategy of a mouse ESC-derived wEB **a.** Representative plot showing a dissociated GFP negative non-virus transduced EB gated for GFP. **b,b'.** Gate showing the percentage of GFP+ cells from ShH10 and AAV2/9 Rhodopsin.GFP+ rod photoreceptors. **c,c'.** Gate showing the percentage of GFP+ cells from ShH10 and AAV2/9 Mopsin.GFP+ cone photoreceptors.

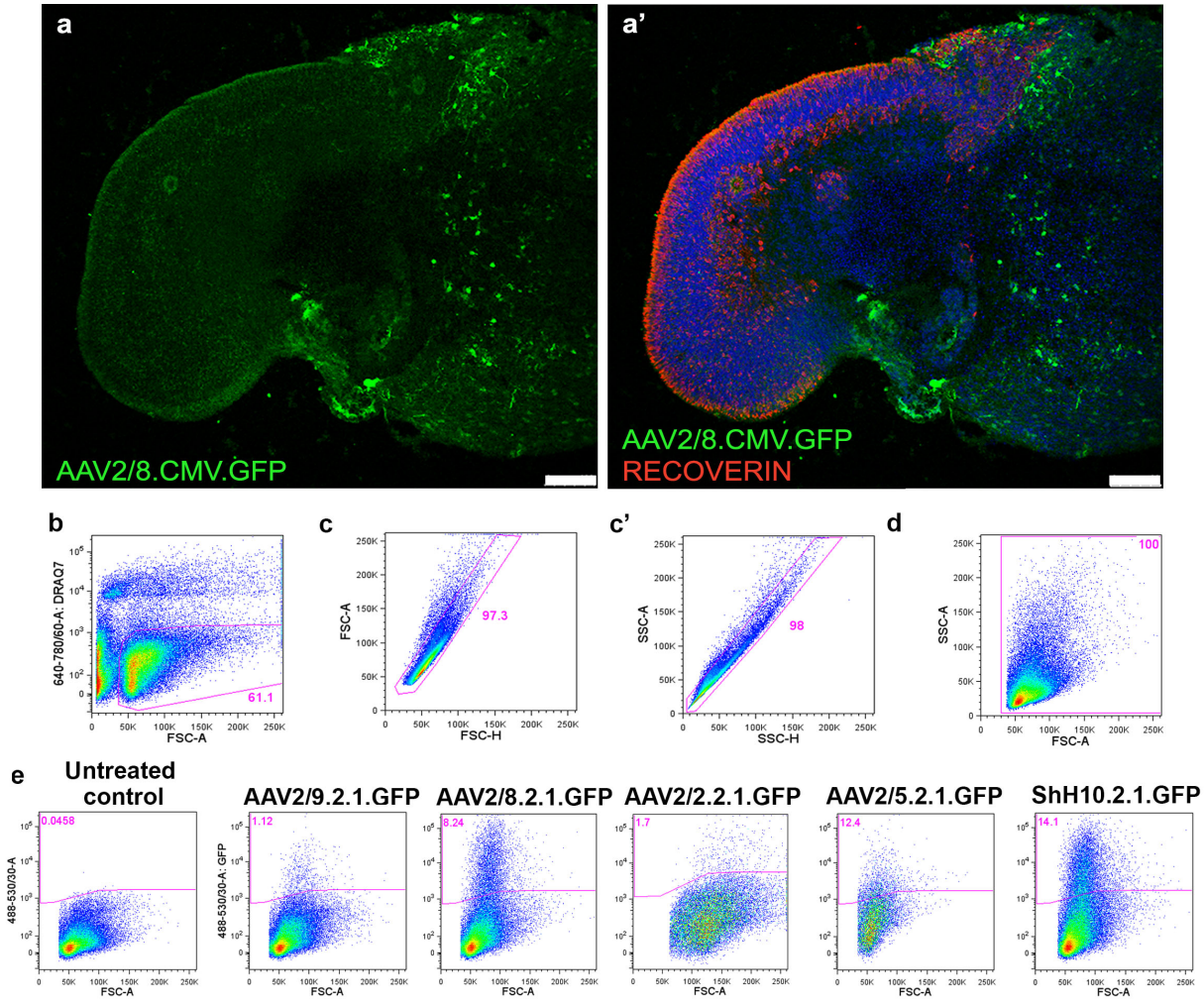

Supplementary Figure S7. Viral transduction efficiency of human ESC-derived photoreceptors

a. Low magnification image showing an AAV2/8.CMV.GFP transduced retinal organoid. RECOVERIN+ (red) photoreceptors neuroepithelia is negative for GFP+. Flow cytometry gate strategy of a human ESC-derived optic vesicle. **b.** Representative plot showing a dissociated

organoids stained for Sytox Blue dead cell stain used to exclude dead cells and cellular debris and identify the live cell population. **c,c'.** Plot showing the exclusion of cellular aggregates to isolate single cells. **d.** Plot depicting the relative size and granularity of single, live cells. **e.** Histograms showing anon-virus treated control and the percentage of GFP+ cone photoreceptors (2.1.GFP) for each of the viruses tested. Nuclei were stained with DAPI (blue). Scale bars: 100μm (**a-a'**).

Supplementary Table 2. Antibodies used for immunohistochemistry

Antigen	Host species	Concentration used	Supplier
Cralbp	mouse	1 in 100	Abcam (15051)
Mitf	mouse	1 in 200	Millipore (MAB3747)
Recoverin	rabbit	1 in 1000	Millipore/Merck (AB5585)
Rhodopsin	mouse	1 in 1000	Sigma (O4886)
Rxrγ	rabbit	1 in 200	Abcam (ab15518)
Sopsin	rabbit	1 in 200	Millipore (AB5407)
Mopsin	rabbit	1 in 200	Millipore (AB5405)
Gnat1	rabbit	1 in 1000	Santa Cruz